CONF-8810155--14
NOV 1988
CONF-8810155--14

DE89 003115

ADVANCES IN CRACK-ARREST TECHNOLOGY FOR REACTOR PRESSURE VESSELS*

B. R. Bass and C. E. Pugh
HEAVY SECTION STEEL TECHNOLOGY PROGRAM
OAK RIDGE NATIONAL LABORATORY
Oak Ridge, TN 37831

ADVANCES IN CRACK-ARREST TECHNOLOGY FOR REACTOR PRESSURE VESSELS*

B. R. Bass and C. E. Pugh
HEAVY SECTION STEEL TECHNOLOGY PROGRAM
OAK RIDGE NATIONAL LABORATORY
Oak Ridge, TN 37831

ABSTRACT

The Heavy-Section Steel Technology (HSST) Program at the Oak Ridge National Laboratory (ORNL) under the sponsorship of the U.S. Nuclear Regulatory Commission is continuing to improve the understanding of conditions that govern the initiation, rapid propagation, arrest, and ductile tearing of cracks in reactor pressure vessel (RPV) steels. This paper describes recent advances in a coordinated effort being conducted under the HSST Program by ORNL and several subcontracting groups to develop the crack-arrest data base and the analytical tools required to construct inelastic dynamic fracture models for RPV steels. Large-scale tests are being carried out to generate crack-arrest toughness data at temperatures approaching and above the onset of Charpy upper-shelf behavior. Small- and intermediate-size specimens subjected to static and dynamic loading are being developed and tested to provide additional fracture data for RPV steels. Viscoplastic effects are being included in dynamic fracture models and computer programs and their utility validated through analyses of data from carefully controlled experiments. Recent studies are described that examine convergence problems associated with energy-based fracture prarameters in viscoplastic-dynamic fracture applications. Alternative techniques that have potential for achieving convergent solutions for fracture parameters in the context of viscoplastic-dynamic models are discussed.

1. INTRODUCTION

The Heavy-Section Steel Technology (HSST) Program at the Oak Ridge National Laboratory (ORNL) under the sponsorship of the U.S. Nuclear Regulatory Commission is continuing to improve the understanding of conditions that govern the initiation, rapid propagation, arrest, and ductile tearing of cracks in reactor pressure vessel (RPV) steels. In pressurized-thermal-shock (PTS) scenarios, inner surface cracks in an RPV have the greatest propensity to propagate because they are located in the region of highest thermal stress,

---

*Research sponsored by the Office of Nuclear Regulatory Research, U.S. Nuclear Regulatory Commission under Interagency Agreement 1886-8011-9B with the U.S. Department of Energy under Contract DE-AC05-84OR21400 with Martin Marietta Energy Systems, Inc.

lowest temperature and greatest irradiation damage. If such a crack begins to propagate radially through the vessel wall, it will extend into a region of higher fracture toughness due to the higher temperatures and less irradiation damage. Because crack initiation is a credible event in a PTS transient, assessment of vessel integrity requires the ability to predict all phases of a fracture event. These phases included crack initiation, nonisothermal propagation, arrest, stable or unstable ductile tearing, and structural instability. Through the integrated efforts of several laboratory and university research groups, the HSST Program is developing various components of the technology required to treat these phases of a fracture event. The technology includes fracture models, analysis methods, criteria and data curves and is being developed and validated through small- and large-specimen experiments.

This comprehensive fracture technology development is addressing several important technical aspects: dynamic fracture-toughness models; rate-dependent data and constitutive models; crack-arrest data and interpretation; transferability of fracture models (e.g., from small to large specimens); cleavage/tearing transition data and modelling guidelines; and least-upper-bound temperature for cleavage behavior. Several of these issues must be studied in the context of inelastic-dynamic fracture models. Until recently, linear-elastic fracture mechanics (LEFM) concepts have been dominant in applications of dynamic analysis techniques [1]. However, except for very short crack jumps, LEFM assumptions may not be strictly valid characterizations of rapid crack propagation [2]. An indication that LEFM conditions are not satisfied occurs when elastodynamic analyses of crack run-arrest data lead to geometry-dependent fracture toughness relations. Recent studies [3] have demonstrated that this geometry dependence can be removed through application of viscoplastic fracture models that incorporate plasticity and strain-rate effects. The importance of viscoplastic effects in dynamic fracture analysis is a key component of the technology under development.

This paper describes recent advances in the coordinated effort being conducted under the HSST Program by ORNL and several subcontracting groups to develop the crack-arrest data base and the analytical tools required to construct inelastic-dynamic fracture models for RPV steels. Experimentally, large-scale tests [4-8] are being carried out to generate crack-arrest toughness data at temperatures approaching and above the onset of Charpy upper-shelf behavior. These tests involve large thermally-shocked cylinders [4], pressurized-thermally-shocked vessels [5,6], and wide-plate specimens [7,8]. The highest number of data points are being generated in these studies by the wide-plate tests [7,8] which are performed at the National Institute of Standards and Technology (NIST) for the HSST Program. These tests are extending the crack-arrest data base for ductile steels to temperatures that are higher than those capable of being imposed in conventional small-specimen tests. It is within the range of this higher temperature data that crack arrest is most likely to occur in a PTS scenario. To substantially augment the data base, crack-arrest toughness data from small- and intermediate-size specimens [9-12] subjected to static and dynamic loading are being generated at Battelle Columbus Division (BCD), ORNL, Southwest Research Institute (SwRI), and the University of Maryland (UM).

Analytically, viscoplastic effects are being included in the dynamic fracture models and computer programs and their utility validated through analyses of carefully controlled experiments. Material properties characterization testing has been performed on A533 grade B class 1 (A533B) steel by Ohio State University (OSU Ref. [13]), SwRI (Ref. [14]), and SRI International (Ref. [15]) using tensile and split-Hopkinson bar techniques. These data have been used to derive material constants for the Bodner-Partom [16], the Perzyna [17] and the Robinson [18] viscoplastic models. These constitutive models, along with crack propagation techniques and several proposed nonlinear fracture parameters, have been installed in HSST-developed finite-element computer programs. Two computer programs [ADINA/VPF (Refs. [19-20]) from ORNL and VISCRK (Ref. [11]) from SwRI] have been developed independently to evaluate different analysis techniques and to insure high-quality dynamic solutions. The capabilities of these nonlinear techniques are being compared and evaluated, in part, through applications to the small- and large-specimen crack run-arrest experiments.

Recent studies indicate that convergence of the leading energy-based fracture parameters (T*, etc.) has not been established for viscoplastic-dynamic fracture applications [21]. Two parallel studies are under way to address the issue of convergence. SwRI is performing studies of the geometry independence of a two-component parameter (T^*, ε) based on a process zone of height 2 ε that extends with the moving crack tip [22]. ORNL is studying a crack propagation model based on a variable-order singular element formulation [23]. Other contributions include asymptotic crack-tip studies being conducted by OSU [24,25]. Additionally, ORNL and UM are determining preliminary relations of crack-tip velocity vs pseudo-K vs temperature for nonlinear fracture conditions. Some details of these recent developments in crack-arrest technology under the HSST Program are described in the following sections.

2. DYNAMIC FRACTURE TESTING PROGRAM

2.1 Wide-Plate Tests

A vital component of the HSST crack-arrest studies is the wide-plate tests which are conducted at NIST. A total of sixteen wide-plate experiments have been performed using two steels. Objectives of these tests are to: (1) extend the existing K_{Ia} data bases to values above the limit in the ASME Code, (2) clearly establish that crack arrest does occur prior to fracture-mode conversion, (3) provide data to improve and validate elastic and visco-plastic-dynamic fracture models, and (4) develop improved experimental dynamic fracture methods. The initial series of wide-plate crack-arrest specimens (WP-1) is taken from a plate of A533B steel that is in a quenched and tempered condition [7]. Drop-weight and Charpy V-notch test data indicate that RT_{NDT} = −23°C, and Charpy upper-shelf energy is 160 J with its onset occurring at about 55°C. The WP-2 series of wide-plate specimens is taken from a plate of 2 1/4 Cr-1 Mo steel that has been heat treated to produce a low upper-shelf Charpy impact energy [8]. Based on a limited number of tests, the tentative drop-weight nil-ductility temperature for the material is >60°C, and the Charpy upper-shelf energy is about 50 J with its onset occurring at about 150°C. Additional material characterization data for the WP-1 and WP-2 series steels can be found in Refs. [7–8].

2.1.1 Test conditions for wide-plate specimens

The 1 by 1 by 0.1 m specimens (1 by 1 by 0.15 m for specimens WP-1.7, WP-1.8, WP-2.1, WP-2.2 and WP-2.3), shown schematically in Fig. 1, were machined and precracked by ORNL. The total crack length for each specimen was nominally 0.2 m (a/W ~ 0.2). Each side of a specimen was side grooved to a depth equal to 12.5% of the plate thickness. Each specimen was welded to pull plates which have a pin-to-pin length of 9.6 m to minimize stress-wave effects. Up to 25 gages have been utilized to provide dynamic strain-field measurements for determining crack velocity and assessing boundary conditions. Thermocouples were positioned on each specimen and sequentially monitored to insure that the desired temperature distribution was achieved throughout the plate assembly.

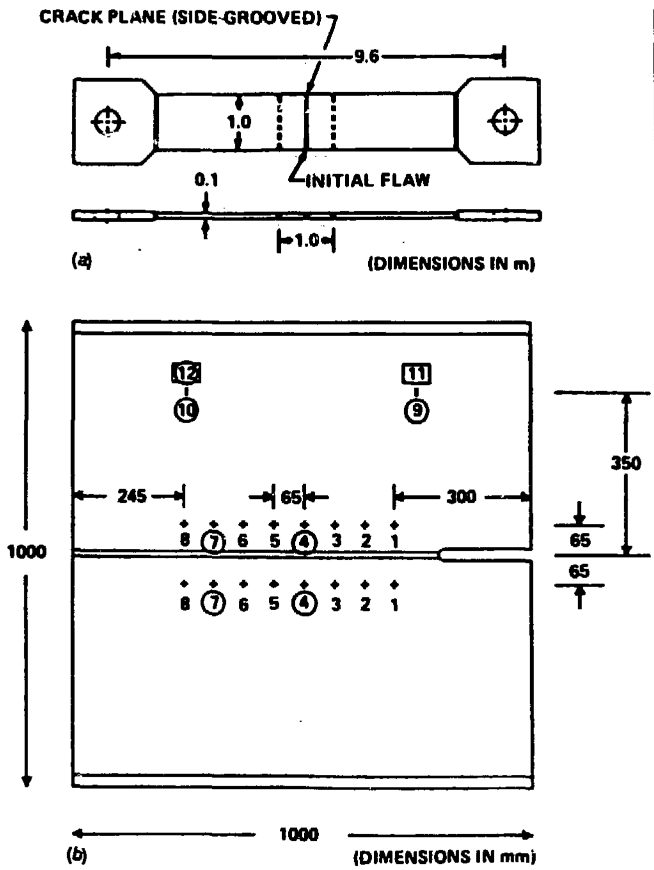

Fig. 1. Wide-plate assembly and crack-arrest specimen: (a) pull-plate assembly; (b) specimen with strain-gage locations.

In each wide-plate test, a fracture toughness gradient was achieved across the plate by LN_2 cooling of the notched edge while heating the other edge. Liquid nitrogen flow and power to the heaters were continuously adjusted to obtain the desired thermal gradient. Tensile load was then applied at a rate of 11 to 25 kN/s until fracture occurred.

2.1.2. Summary of posttest analysis results

A summary of conditions for each test in the WP-1 and the WP-2 series is given in Ref. [8]. Posttest elastodynamic fracture analyses were conducted for each wide-plate test to investigate the interaction of parameters that affect the crack run-arrest events. Figure 2 summarizes crack-arrest toughness values for the WP-1 and WP-2 series which were computed in fixed-load, generation-mode dynamic finite-element analyses. (In the generation-mode analysis, the crack tip is propagated according to a prescribed crack position vs time relation obtained from measured data.) Results for both test series exhibit a significant increase in toughness at temperatures near and above the onset of Charpy upper shelf ($T - RT_{NDT}$ = 78°C for WP-1; $T - DW_{NDT}$ = 90°C for WP-2). Crack-arrest toughness values obtained from this series of tests extend consistently above the ASME reference fracture-toughness curve. The increase in arrest-toughness values which occurs at an accelerating rate with temperature near and above the onset of Charpy upper shelf suggests that a

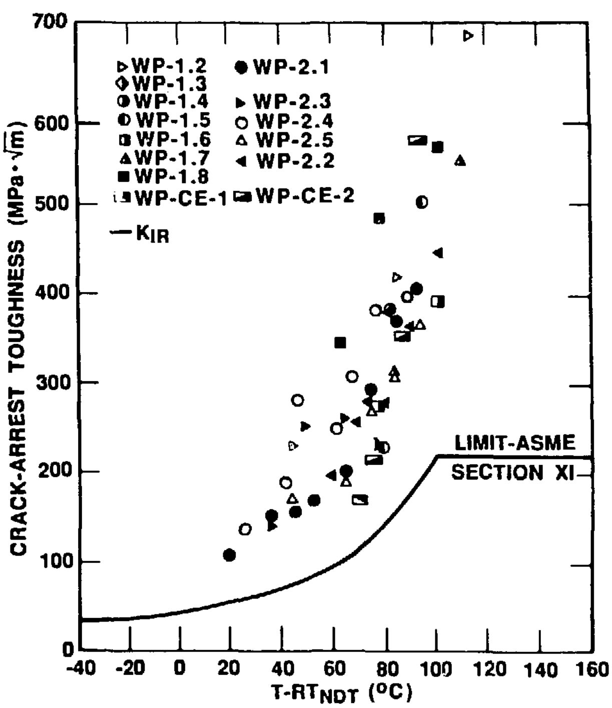

Fig. 2. Generation-mode (fixed load) crack-arrest toughness data versus temperature ($T - RT_{NDT}$) for HSST wide-plate tests.

temperature limit exists at or below which cleavage crack propagation will arrest, no matter how high the applied driving force. Results presented in Fig. 2 also show that arrest of cleavage crack propagation can and does occur at temperatures above the onset of Charpy upper shelf.

The importance of the analysis method (static vs dynamic) and boundary conditions (fixed load or fixed load-pin displacement) utilized to interpret the wide-plate crack-arrest tests is demonstrated by comparing the values given in Fig. 3 for specimen WP-2.4. Values of K_{Ia} determined using the secant equation [26] and the Tada fixed load condition [27] represent approximate lower and upper bounds, respectively, to the dynamic results in Fig. 3. For long-duration crack run-arrest events (>20 ms), such as could occur for the low Charpy upper-shelf material, considerable load adjustment can take place as a result of specimen/pull-plate compliance. Therefore, the most meaningful values of K_{Ia} under such conditions must reflect this occurrence and involve a dynamic finite-element analysis. The dynamic generation-mode (fixed load) analysis results represent one such calculation.

Predictions of crack propagation and arrest in dynamic fracture problems requires specification of the relation among instantaneous crack-tip velocity, $\dot{a}$, dynamic fracture toughness, K_{ID}, and temperature, T, for the fracturing material. This relation is a primary input for predictive application-mode dynamic fracture analyses. [In an application-mode analysis, the crack tip is propagated incrementally when the relation $K_{applied} = K_{ID}(\dot{a}, T)$ is satisfied.] At UM, Schwartz [28] has used data from the WP-1 series of

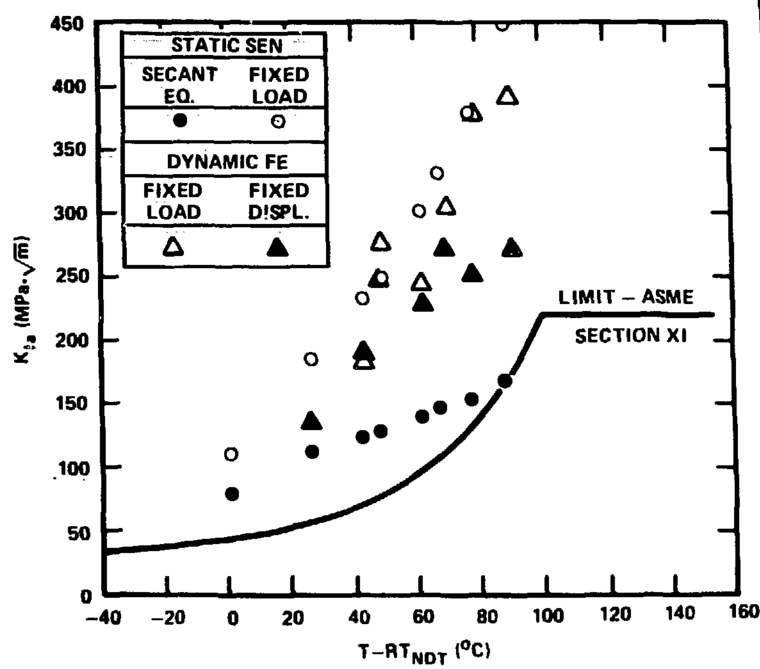

Fig. 3. Static and dynamic crack-arrest toughness determination vs temperature (T – RT_{NDT}) for specimen WP-2.4.

wide-plate tests to estimate the $\dot{a}$ vs K_{ID} vs T relation for A533B steel given in Fig. 4. The toughness relation in Fig. 4 has been used by ORNL for pretest analysis of intermediate-size crack-arrest specimens [10] of A533B steel.

Topographic analyses of selected wide-plate fracture surfaces are being performed at UM using stero-SEM and relative-height measurement techniques. In Ref. [12], these techniques were applied to regions of fracture surfaces (from WP-1.7 and WP-CE-1) where cleavage arrest was followed by fibrous-tearing reinitiation. Estimates of crack-tip opening displacement (CTOD) obtained from relative-height measurements were used to calculate K_I-values at reinitiation. These studies indicated that high K_I-values (>350 $MPa\sqrt{m}$) were necessary to initiate fibrous tearing from an arrested cleavage crack in the upper transition temperature range. It is anticipated that large uncertainties in these topographic estimates of K_I at reinitiation can be reduced substantially by improving the topographic mapping of the regions of interest.

More refined analyses of the wide-plate test data will be performed by ORNL and UM to determine the influence of tunneling on computed crack-arrest toughness values. To address this issue, the relevant experimental and analytical literature on crack tunneling will be reviewed and a series of

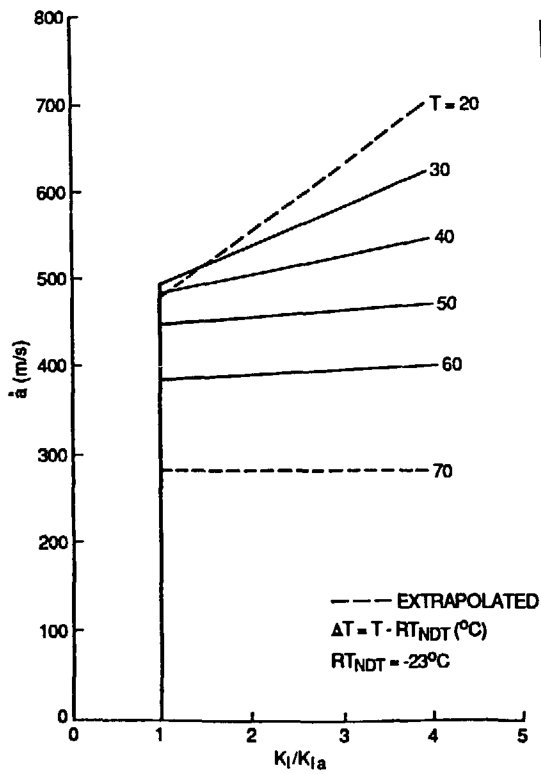

Fig. 4. Crack-tip velocity vs dynamic stress-intensity factor vs temperature inferred from A533B steel.

three-dimensional studies of crack tunneling will be performed under quasi-static conditions. The major thrusts of these investigations will be to develop a more refined analytical model for tunneling and to determine any necessary corrections to the wide-plate test results to account for the influence of tunneling.

2.2 Pressurized-Thermal-Shock Experiment (PTSE-2)

The HSST Program is obtaining additional crack-arrest data through pressurized-thermal-shock tests [5,6] that provide validation data under multiaxial transient conditions. The PTS experiments are the most recent of a long succession of validation experiments that are on a sufficiently large scale to allow important aspects of the fracture behavior of nuclear reactor pressure vessels to be simulated. Elastodynamic finite-element analyses [29] were previously carried out for the two cleavage crack run-arrest events that occurred in the second and third phases of the PTSE-1 test [5]. The dynamic results showed good agreement between data and predictions for the short crack runs of that experiment, and quasi-static and dynamic analyses showed little difference. These same dynamic fracture analysis techniques have been applied now to the analysis of the two crack run-arrest events of PTSE-2 [6].

2.2.1 Test conditions for PTSE-2

Dimensions of the test vessel and flaw geometry are given in Table 1 for the PTSE-2 test [6]. An HSST Intermediate Test Vessel (ITV) was used as a tough carrier vessel and prepared with a plug of test steel welded into the vessel. The test material was a specially heat treated 2 1/4 Cr-1 Mo plate with a low Charpy upper-shelf energy (~50 to 70 J) and low ductile-tearing resistance. The 1-m-long sharp flaw was implanted in the outside surface of the plug by cracking a shallow electron-beam weld under the influence of hydrogen charging. For each test, the ITV was extensively instrumented to give direct measurements of crack-mouth opening displacement, temperature profiles through the vessel wall, and internal pressure during the transient. In the experiment, the flawed vessel was enclosed in an outer vessel that was electrically heated to bring it to the desired uniform initial temperature of about 290°C. A thermal transient is initiated by suddenly injecting chilled

Table 1. Geometric parameters of PTSE-2 vessel

Inside radius	=	343 mm
Wall thickness (w)	=	147.6 mm
Flaw length	=	1000 mm
Flaw depth (a)	=	14.5 mm
a/w	=	0.098 mm

water (or a methanol-water mixture) through an annulus between the test vessel and the outer vessel. Extensive material properties testing of the vessel insert material preceded the PTS experiment. The tensile strength was undesirably low, but other properties, although somewhat uncertain, were satisfactory. Some of the properties determined prior to the experiment are summarized in Table 2.

Table 2. Properties of PTSE-2 vessel insert material

Yield strength	= 255 MPa
Ultimate strength	= 518 MPa
NDT temperature	= 49°C
Onset of Charpy upper shelf (100% shear fracture appearance)	= 150°C
Charpy upper-shelf energy	= 50–75J[a]

[a]Range for all depths in plate. The average at 1/4 depth is 68 J.

The experiment was planned to consist of two transients, of which the first would induce warm prestressing ($\dot{K}_I < 0$) followed by reloading ($\dot{K}_I > 0$) until the crack propagated by cleavage. The second transient was planned to produce a deep cleavage crack jump with an arrest or mode conversion occurring only after conditions conducive to unstable tearing were attained. In the first transient PTSE-2A, ductile tearing occurred in three separate phases: (1) prior to warm prestressing; (2) during reloading; and (3) after the cleavage arrest. The crack propagated both axially and radially by cleavage. In the second transient PTSE-2B, K_I increased monotonically, while the crack tore stably, propagated radially in cleavage, and then tore unstably.

2.2.2 Summary of posttest analysis results

In the elastodynamic analyses of the transient observed in PTSE-2, a 2-D plane strain finite-element formulation was utilized to model the test vessel. The finite-element model and the material properties utilized in this analysis are described in Ref. [30]. Measured values of the radial temperature distribution and internal pressure at the time of cleavage crack propagation in the transient of PTSE-2 are given in Ref. [6]; the boundary conditions are assumed constant during the run-arrest event.

Results from application-mode elastodynamic analyses of the A and B transients are depicted in Figs. 5 and 6 and in Table 3. Figure 5 gives the computed crack-depth ratio, a/w, as a function of time for each of the two transients and compares computed values with measured data at crack arrest.

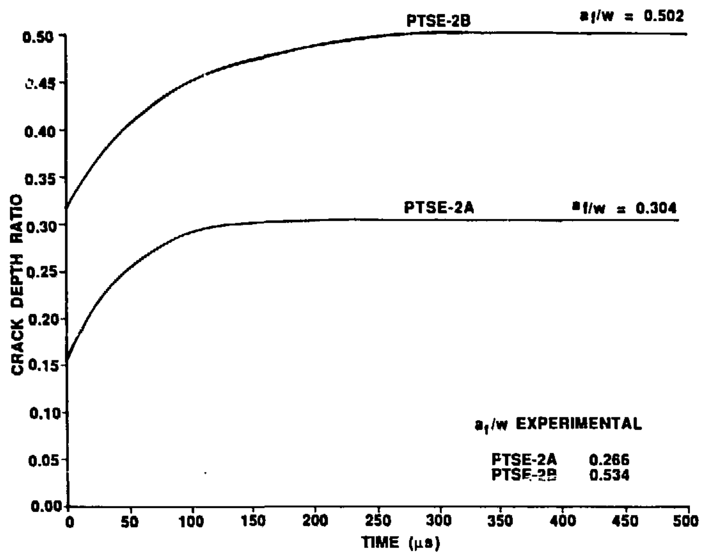

Fig. 5. Crack-depth ratio versus time for posttest elastodynamic analysis of PTSE-2.

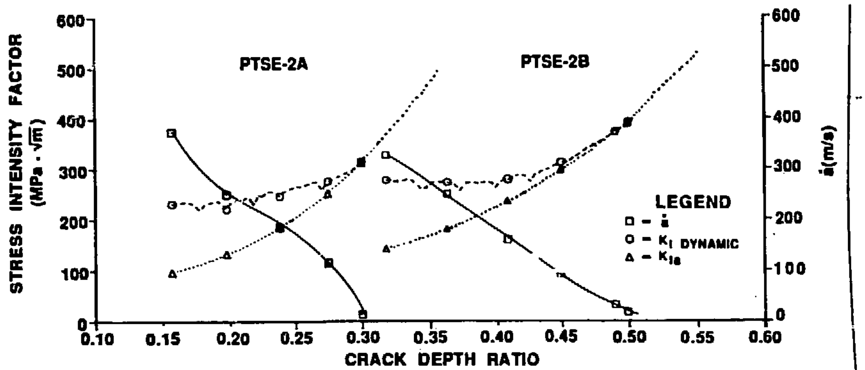

Fig. 6. Stress-intensity factor, crack-velocity, and static crack-arrest toughness versus crack-depth ratio for posttest elastodynamic analysis of PTSE-2.

Figure 6 depicts the dynamic stress-intensity factor, K_I, the crack velocity, $\dot{a}$, and the static crack-arrest toughness, K_{Ia}, vs a/w relations for the transients, and it indicates that the crack propagates into a rising K_I field for both run-arrest events. Table 3 compares selected results from previously reported 2-D quasi-static elastoplastic analyses [6] based on measured crack depths and from the quasi-static elastic and elastodynamic analyses of the present study. The differences in computed K_I values at initiation in the two transients are due primarily to plasticity effects that are not modelled in this study.

Table 3. Initiation and arrest parameters from posttest elastoplastic and elastodynamic analyses of PTSE-2

Experiment phase	a/w	a (m)	Temperature (°C)	K_I (MPa$\sqrt{m}$)	Event
PTSE-2A					
S[a]	0.1524	0.0225	80.7	198.9	Initiation
ES[b]	0.1524	0.0225	80.7	238.4	Initiation
S	0.2663	0.0393	130.6	261.4	Arrest
ED[c]	0.3040	0.0449	145.6	313.8	Arrest
PTSE-2B					
S	0.3123	0.0461	102.4	248.1	Initiation
ES	0.3123	0.0461	102.4	284.5	Initiation
S	0.5339	0.0788	162.9	419.3	Arrest
ED	0.5016	0.0740	155.4	393.2	Arrest

[a]S = quasi-static elastoplastic analyses (Ref. [6]) based on measured crack depth.

[b]ES = quasi-static elastic analysis (Ref. [30]).

[c]ED = application-mode elastodynamic analysis (Ref. [30]).

The computed results presented in Figs. 5 and 6 represent contrasts in the predicted kinematic behavior of the crack tip during the two transients of PTSE-2. In the A transient, the computed crack-tip velocity falls rapidly to zero at time t ≈ 150 μs following initiation of the cleavage event. Calculations for the B transient indicate that the crack velocity was non-zero for a longer period of time, at least 300 μs. The cleavage event observed in the B transient was interrupted by a narrow band of ductile tearing at a/w ≈ 0.47 that extended the entire length of the crack. Posttest studies of the fracture surface indicate that cleavage was still occurring over short discontinuous segments of the tearing band, and that the crack eventually reinitiated in cleavage and arrested at a/w = 0.534. Although the complex interactions of these fracture modes are not modelled in the present study, results in Fig. 6 show that a small increase in the K_{Ia} curve could produce an arrest at the approximate location of the ductile tearing band. No such interruption of the A transient cleavage event by tearing was detected, and the computed results in Fig. 6 are consistent with that observation.

Results presented in Fig. 3 show that the wide-plate K_{Ia} test results exhibit an accelerating increase in arrest-toughness values with increasing temperature. The trend for K_{Ia} values to extend consistently above the limit provided in ASME Section XI is further substantiated in Fig. 7 which presents data from the PTS and wide-plate experiments and from other large-scale tests summarized in Ref. [8].

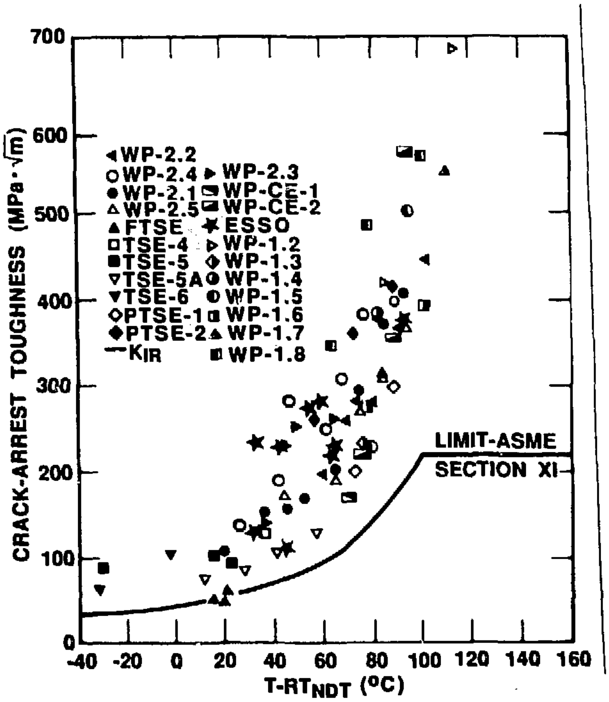

Fig. 7. High-temperature crack-arrest toughness data vs temperature ($T - RT_{NDT}$) for wide-plate, PTS, and large-specimen tests.

2.3 Intermediate- and Small-Scale Specimen Tests

2.3.1 Stub-panel crack-arrest specimen

Studies [10] have been conducted by the HSST Program at ORNL to evaluate the usefulness of crack-arrest experiments that employ a relatively small panel specimen whose size is between conventional crack-arrest specimens and the wide-plate specimens. For the design of the specimen geometry, the following requirements were adopted:

1. measurement of crack-arrest toughness values >200 MPa•√m,
2. measurement of toughness values in a rising field of stress-intensity factor, and
3. a limit capacity of 2.5 MN for the available testing machines.

The stub-panel specimen (45.1 × 99.1 × 3.39 cm) depicted in Fig. 8 was proposed to meet the above requirements. The plate is side-grooved to a depth of 12.5% of the thickness, resulting in a net thickness of 2.54 cm at the crack plane. A gradient in fracture toughness is achieved by cooling the stub region and heating the panel edge to produce a nonuniform steady-state temperature distribution across the plate. A tensile load is applied to the panel to produce a rising driving force. The stub is mechanically loaded to provide

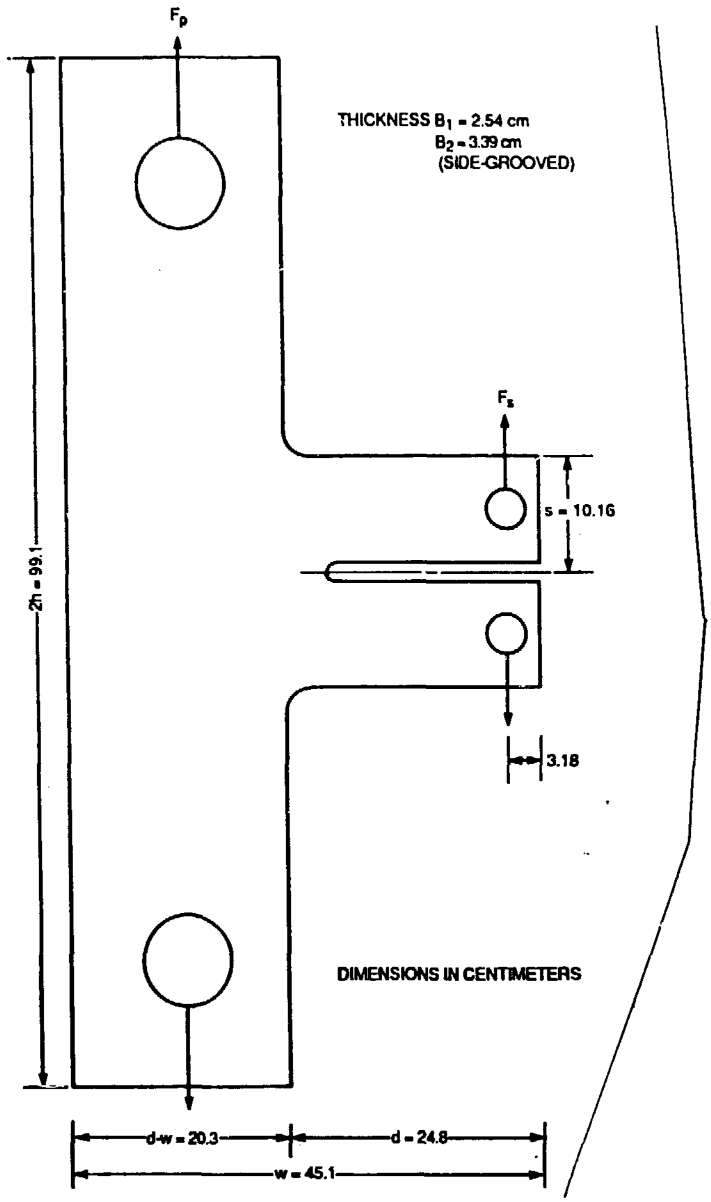

Fig. 8. Geometry and loading system of stub-panel crack-arrest specimen.

K_I levels that are high enough for initiation of the chilled crack in cleavage. Arrest of the fast-running crack then occurs in the ductile high-temperature region of the panel. Static and dynamic analyses [10] were carried out for the stub-panel configuration to assess its utility for producing K_{Ia} data in the temperature regime of upper-shelf material behavior. These analyses indicated that crack-arrest toughness values >200 $MPa \cdot \sqrt{m}$ could be measured in a rising K_I field by using available testing machines and appropriate thermal boundary conditions.

Plans have been formulated at ORNL for fabricating, instrumenting, and testing the stub-panel specimen in Fig. 8. The first specimen was fabricated from the same plate (HSST plate 13-A) of A533B steel as that used in the WP-1 series of wide-plate tests. Material properties for the test plates have been described previously in Ref. [10]. To record pertinent data during the test, the specimen will be instrumented with thermocouples, strain gages, and displacement gages, using a placement configuration and instrumentation chain similar to that employed for the wide-plate specimens [7]. The first specimen will be tested early in FY 1989.

2.3.2 Small dynamic-fracture specimens

Crack-arrest toughness data applicable to PTS conditions is being developed through small-scale specimen testing programs by several HSST subcontracting institutions. At SwRI, experimental research [31] has been directed toward obtaining dynamic crack-propagation data in A533B steel using small-scale specimens supplied by ORNL. For this purpose, a series of duplex A533B/4340 steel specimens of effective width, w = 127 mm, were instrumented and tested at 23°C. Crack growth was monitored on both surfaces of each specimen using crack gages, whereas crack-line displacement was measured using an eddy-current transducer. Dynamic-strain measurements were also obtained and used to examine the detailed interaction between stress-wave propagation and crack-growth response. Results from dynamic analyses performed with the SwRI code VISCRK have been reported for two duplex experiments (SD2 and SD6) in Ref. [31]. Figure 9 shows the K_{Ia} values from these analyses plotted with the ORNL equation for K_{Ia} and the ASME K_{IR} curve. Similarly, the K_{Ia} values for SwRI analyses of the first crack-extension event in several of the WP-1 series of wide-plate experiments are shown in Fig. 9.

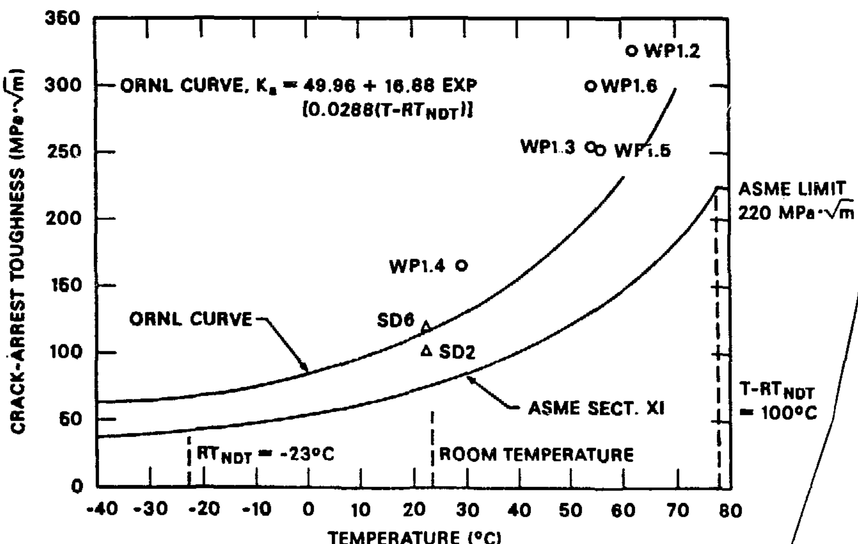

Fig. 9. Crack-arrest toughness data vs temperature for SwRI duplex specimen tests and HSST wide-plate tests.

A new technique developed at SwRI enables two relatively small specimens to be tested simultaneously using stress-wave loading from Hopkinson-type pressure bars [31]. Precracked compact-type A533B steel specimens, without side-grooves and having an effective width w = 44 mm, have been tested at 23 and 37°C. Crack growth of ~15 mm was achieved. Two A533B specimens with side-grooves and a modified fastening mechanism to the pressure bars are being prepared for testing at temperatures ranging from 37 to 50°C.

At UM, efforts have focused on the development of two different rapid loading fracture experiments [12]. The goal of one of these studies is to determine the limits of approximating the crack-arrest toughness, K_{Ia}, by the dynamic initiation-toughness, K_{Id}. In the latter case, explosively-loaded notched short-bars are being tested and the K_{Id} values so obtained are compared with K_{Ia} values for the same material. In the other study, a method is being developed to measure "lower bound" cleavage initiation-toughness in the transition temperature range using a small specimen. A notched round-bar subjected to impact loading is being used for the latter study.

Feasibility studies demonstrated that photoelastic and strain-gage techniques could be employed to measure K_{Id} in the notched short-bar specimens. The loading of the short bar with its integral dog-bone ends is accomplished with four explosive charges that are detonated simultaneously. Tensile stress waves produced at each end of the bar propagate to the central region of the bar, where they combine to produce a rapidly increasing K_I field that initiates a stationary crack.

The first two notched short-bar specimens were fabricated from 12.7-mm-thick 4340 steel hardened to R_c = 51, with a fatigue-sharpened crack 17.5 mm deep used as an initiator. The first test indicated that symmetric loading was achieved and the central crack extended straight across the midsection of the bar. Strain gage records were successfully obtained in the second test, and indicate a dynamic initiation-toughness K_{Id} = 53.0 MPa$\cdot\sqrt{m}$. The next series of tests will focus on specimens of A533B steel subjected to very high rates of loading. These specimens will be extended to a length of 400 mm in the straight-bar region to move the crack-tip strain gages away from the explosive charges and to allow more time for the loading wave to propagate to the center notch.

The impact-loaded notched round-bar experiment was developed by UM in an attempt to simulate the effects of constraint of a very thick specimen with a relatively small round bar. The cylindrical shape of the bar should increase the effective thickness of the specimen by a factor of ~3. The specimen configuration used in testing consists of a notched bar with outside diameter of 38.1 mm and a machined notch of diameter 19.1 mm. The notch is machined with an overly sharp Charpy notch-cutting tool with a notch tip radius of 0.127 mm. The loading system designed to apply impact loading to these specimens is capable of delivering 1051 J of energy when the weight of 58.8 kg drops through a distance of 1.83 m. Initial experiments made with strain-gaged specimens indicate that nominal strain rates approach 20 s^{-1} with this system. However, the actual strain rate at the notch is much higher because of the 4/1 area ratio and because of the large strain concentration that occurs at the tip of the root radius.

In the first test series, five specimens of A508 steel were tested under axial impact loading applied by dropping the 58.6 kg weight a distance of 1.78 m. All five specimen failed, and data obtained for the determination of K_{Id} were found to be consistent and repeatable, yielding an average value of $K_{Id} = 54\ MPa\sqrt{m}$. For the next series of tests, twenty notched round-bar specimens are being machined from A533B steel. These specimens will be tested under impact loading for a range of temperatures to determine the change in initiation toughness from the lower to the upper shelf.

3. INELASTIC FRACTURE MODEL DEVELOPMENT

The basic postulate of LEFM requires that the inelastic deformation surrounding the crack tip be contained within the K_I-dominant region. Furthermore, it is assumed that rapid crack propagation is governed by a unique geometry-independent material property, the dynamic fracture toughness, K_{ID}. Propagation of a running crack occurs under the condition that the applied dynamic stress-intensity factor, K_I, satisfies $K_I = K_{ID}(\dot{a},T)$, where K_{ID} is taken to be a function of the crack-tip velocity, $\dot{a}$, and the temperature, T. However, except for very short crack jumps, LEFM assumptions may not be strictly valid characterizations of rapid crack propagation [2]. In particular, a wake of residual plasticity left behind the moving crack tip can violate the K_I-dominance requirement of LEFM. An indication that LEFM conditions are not satisfied occurs when elastodynamic analyses of crack run-arrest data lead to geometry-dependent fracture toughness relations. Dahlberg, et al. [32] performed elastodynamic fracture analyses using crack run-arrest data from tests of single-edge-notched (SEN) tension panel specimens of different lengths. Their results for different panel lengths coincide for low crack velocities, but show a definite geometry dependence at higher velocities where non-linear effects are more pronounced. However, Brickstad [3] has demonstrated that this geometry dependence can be removed through application of an inelastic fracture model that incorporates plasticity and strain-rate effects (i.e., viscoplasticity).

These studies indicate that strain-rate effects ($\sim 10^4\ s^{-1}$) can be important for rapid loading situations such as cleavage crack propagation events in ductile RPV steels. The HSST Program research efforts at ORNL and several subcontracting groups are supporting the development of viscoplastic-dynamic finite-element analysis techniques and validating their utility through analyses of carefully controlled experiments. Various viscoplastic constitutive models and several proposed nonlinear fracture criteria have been installed in general purpose (ADINA/VPF) [19,20] and special purpose (VISCRK) [11] finite element computer programs. The constitutive models include the Bodner-Partom [16], the Perzyna [17] and the Robinson [18] viscoplastic formulations; the proposed fracture criteria include three parameters, $\{T^*$ from Ref. [33], $\hat{J}$ from Ref. [34], and γ from Ref. [3]$\}$, that are based on energy principles.

3.1 Viscoplastic Material Model Characterization

Research efforts at ORNL and several subcontracting groups are directed toward developing strain-rate and temperature-dependent constitutive models for A533B steel. These models will be used in dynamic fracture analyses to assess the effect of viscoplastic material behavior on cleavage crack propagation and arrest in RPV steels. As part of this effort, dynamic stress-strain data have been generated by OSU, SwRI, and SRI for A533B steel for use in deriving constants for proposed constitutive models. Kanninen et al. [14] obtained dynamic stress-strain data from tensile and split-Hopkinson bar tests for strain rates ranging from 0.001 to 550 s^{-1} and for temperatures ranging from -60 to 175°C. To augment this data base, Giovanola and Klopp [15] recently performed 15 split-Hopkinson torsion-bar experiments at engineering shear strain rates ranging from 400 to 3000 s^{-1} and at temperatures of -60 to 150°C. Using similar test procedures, Gilat [13] has conducted tests at strain rates of ~800 and 5000 s^{-1} and at temperatures of -150 to 20°C. (All specimens for these tests were taken from HSST Plate 13-A, which is the same source plate for the wide-plate crack-arrest specimens). Results for these tests show that both temperature and strain rate have a significant effect on the material response of A533B steel.

Kanninen et al. [14] used dynamic stress-strain data to derive constants for the Bodner-Parton constitutive model appropriate for A533B steel at test temperatures ranging from -60 to 150°C. At ORNL, Chang [35] has employed stress-strain data from Refs. [14–15] and an extended version of the Robinson model to represent the viscoplastic behavior of A533B steel. The extended Robinson model was originally developed to describe strain-aging effects [36] as exhibited by the phenomena of yield drop for Inconel 617 at 950°C and the reverse strain-rate effect for type 304 stainless steel at 550°C. As illustrated in Fig. 10, the Robinson model effectively models the yield drop

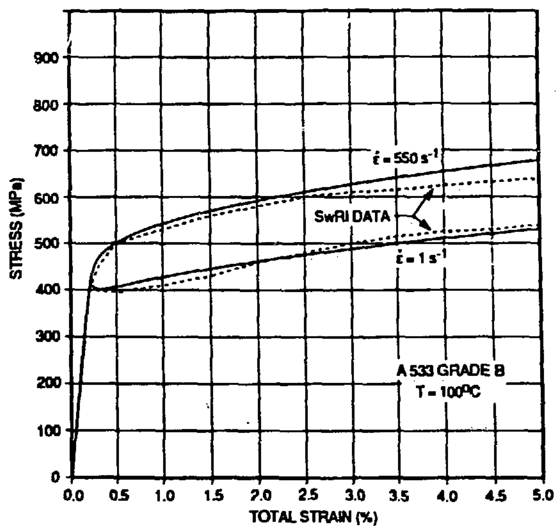

Fig. 10. Comparison of extended Robinson constitutive model predictions with measured stress-strain data for A533B steel at a temperature of 100°C and strain rates of 1 and 550 s^{-1}.

and strain-rate sensitivity of the A533B steel at 100°C. Numerical implementation of the extended Robinson model into ADINA/VPF following a technique due to Hornberger [37] is currently under way at ORNL. Also, the SwRI stress-strain data for A533B steel has been employed by Brickstad [38] to characterize a Perzyna viscoplastic formulation based on the von Mises yield criterion with linear strain hardening.

3.2 Applications of Viscoplastic Analysis Methods

The predictive capabilities of the nonlinear techniques described in the previous section are being evaluated through applications of the ADINA/VPF and VISCRK computer programs to analyses of HSST crack-arrest exeriments. Recently, viscoplastic-dynamic fracture analyses [39] of wide-plate tests WP-1.2 to WP-1.7 were conducted with the ADINA/VPF program at ORNL using finite-element models having improved mesh refinement near the plane of crack propagation. The finite-element model used to analyze tests WP-1.2 to 1.6 is shown in Fig. 11(a); the model used for test WP-1.7 is shown in Fig. 11(b). Both models consist of 2258 nodes and 715 eight-noded isoparametric elements. The dimensions of the elements along the crack path in Fig. 11 are 20 by 20 mm.

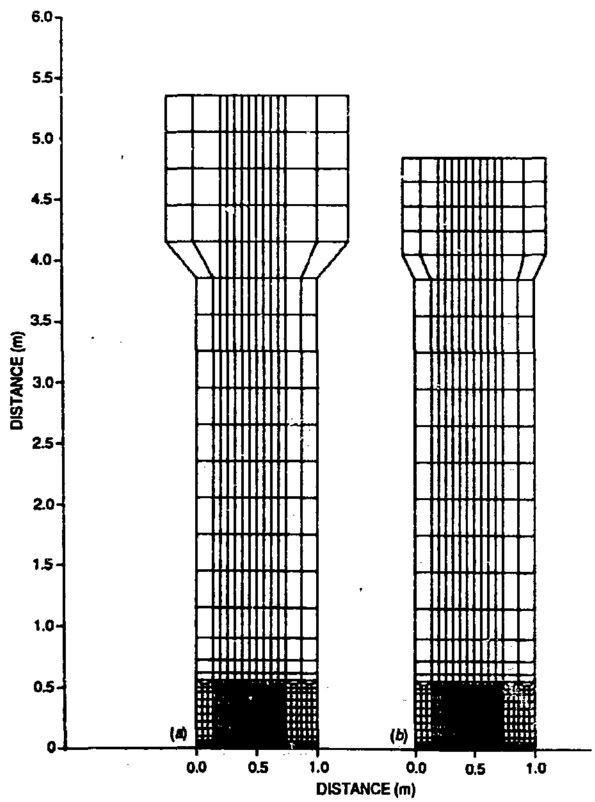

Fig. 11. Finite-element models used in dynamic analyses of tests WP-1.2 through WP-1.7: (a) model of WP-1.2 through WP-1.6, and (b) model of WP-1.7.

From Ref. [39], a generation-mode analysis of wide-plate test WP-1.2 was performed utilizing the estimate of crack position vs time from Fig. 12 and the Bodner-Partom model from Ref. [14]. The crack position vs. time relation in Fig. 12 was constructed in part from strain-gage data recorded at the crack-line strain-gage locations identified in Fig. 1. Figure 12 shows the two measured crack arrests at a_{fm_1} = 0.55 m and at a_{fm_2} = 0.65 m which occurred at times t_{m_1} = 0.96 ms and at t_{m_2} = 2.7 ms after crack initiation, respectively.

Figure 13 compares results from this analysis with those obtained from other models having different mesh refinements along the crack plane. The

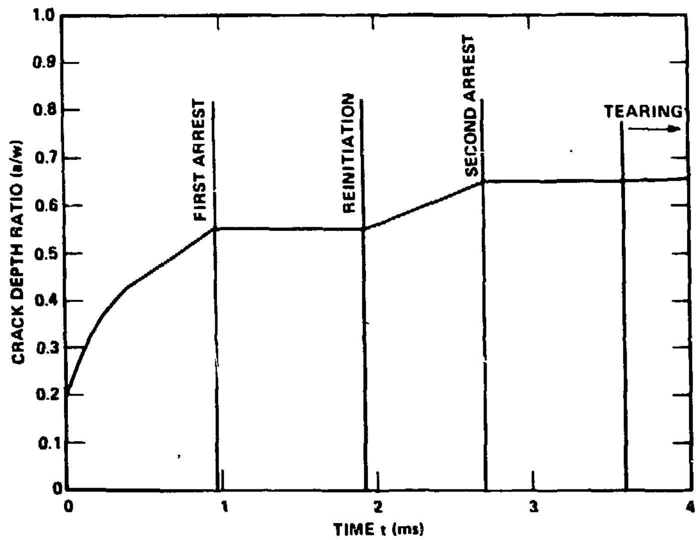

Fig. 12. Crack-depth history derived from strain-gage data for wide-plate test WP-1.2.

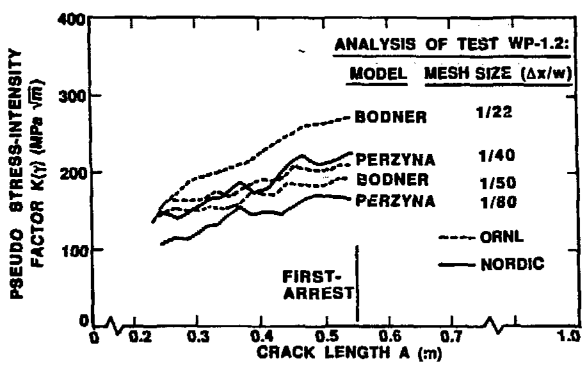

Fig. 13. Comparison of results [$K_I(\gamma)$ vs crack depth] from generation-mode viscoplastic-dynamic analyses of test WP-1.2 for four crack-path mesh refinements.

results are expressed in terms of pseudo-K_I values computed from the rate-of-work function γ (Ref. [3]) and plotted vs. crack length for the first run/arrest event. The characteristic mesh size is defined as the ratio of the crack-path element width to the plate width. The ORNL analysis results shown in Fig. 13 for mesh sizes 1/22, 1/40 and 1/50 were obtained from ADINA analyses described in Refs. [21], [20] and [39], respectively. Also shown in Fig. 13 are results obtained by Brickstad [38] at the Swedish Plant Inspectorate (SA) using mesh sizes 1/40 and 1/80 and the Perzyna viscoplastic model. These combined results indicate that the viscoplastic-dynamic solutions of the wide-plate test expressed in terms of the inelastic fracture parameters (T^*, $\hat{J}$, and γ) have not yet converged for the mesh refinements employed thus far in these studies.

Insight into the difficulties associated with modeling rapid crack propagation events in RPV steels exhibiting viscoplastic behavior are provided by several recent studies. Ahmad [40] employed an asymptotic analysis by Freund and Hutchinson [41] for steady-state crack growth in an elastic-viscoplastic material under small scale yielding to study an HSST wide-plate test specimen. To accurately model the high-strain-rate zone, Ahmad [40] estimates that the element size in the crack-tip region of the wide-plate model should be approximately 1 mm, or $\sim 10^{-3}$ of the planar specimen dimensions. (Thus far, HSST wide-plate analyses have been limited to elements with dimensions greater than 10 mm.) More recent studies by Sheu [24] and by Popelar [25] indicate that the high strain-rate zone is even smaller. Sheu [24] studied the mode I plane strain problem of dynamic steady-state crack growth in A533B steel using the Bodner-Partom model characterized in Ref. [14] and the assumption of small-scale yielding. Focusing on the immediate area surrounding the elastic-plastic boundary, Sheu [24] resolved the near crack-tip singular fields using a finite-element model with element dimensions approximately 10^{-3} of the elastic-plastic zone size. (For the Bodner-Partom model, the stress field is $r^{-1/2}$ singular and the elastic strain rates dominate the plastic strain rates near the crack tip.) In Fig. 14, Popelar [25] has elaborated further on the study of Sheu [24] by estimating the size of the zone-of-dominance of the

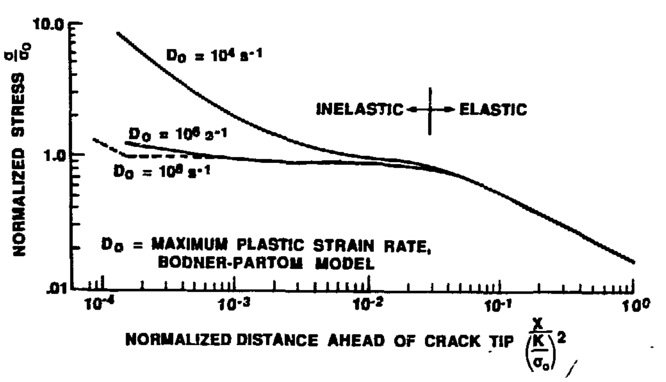

Fig. 14. Variation of effective stress ahead of crack tip as a function of limiting plastic strain rate, D_o, in Bodner-Partom model.

near-tip fields for values of the limiting plastic strain rate as high as $D_o = 10^8\ s^{-1}$. The zone-of-dominance becomes smaller for increasing values of Do and is approximately 10^{-3} of the plastic zone size for Do = $10^8\ s^{-1}$. Furthermore, for A533B steel over a temperature range from −60 to 100°C and a crack speed of one-half the Rayleigh wave speed, Popelar [25] estimates that the zone-of-dominance extends from ~5 to 55 μm compared to an inelastic region with dimensions 0.1 to 15 mm. Representative data for A533B wide-plate material lists grain sizes at ASTM 7-8 corresponding to average diameters from ~27.5 μm to 19.8 μm, respectively [7]. Given that the computational capacity were available to resolve such a small region using finite elements, it is clear that elements of this size invade the micro-heterogeneity of the material and broach the limits of isotropic continuum analysis.

Several techniques are being explored to circumvent these stringent requirements on crack-tip mesh refinement and related difficulties associated with possible violations of continuum assumptions. Motivated by the objective of computing a convergent non-zero value of T*-integral for viscoplastic models, Nishioka [22] has proposed an exclusion zone technique that obviates the need for highly-refined crack-tip elements. In the viscoplastic calculations, a small-rectangular domain of height 2 ε is defined around the crack tip to approximate a finite fracture process zone. Typically this zone is chosen such that ε equals the height of one or two rows of elements along the plane of crack propagation in the finite element model. During the dynamic analysis, this rectangle is extended in length (but not in height) to include a portion of the plastic wake behind the advancing crack. Nishioka [22] advocates excluding the integration of the volume term of the T*-integral (see Ref. [33]) from this extending exclusion zone. According to a study by Nishioka [22], the T*-integral should be essentially invariant with respect to the size of this extending domain provided ε is sufficiently small.

To investigate the potential of the foregoing technique for characterizing fracture behavior, O'Donoghue [42] has performed studies of the geometry independence of the two-component parameter (T*, ε) using a center-crack panel problem (Fig. 15). The panel had dimensions 2 w × 2 h × t (w = 40 mm, h = 20 mm and t = 25.4 mm) with an initial crack length of a/w = 0.25. A fixed load was applied that produced a nominal stress of 300 MPa and an initial stress-intensity factor of $K_I(T^*) = 77\ MPa\sqrt{m}$. The panel was analyzed dynamically as a plane stress problem using the Bodner-Partom model [14] for a constant crack velocity of $\dot{a}$ = 1000 m/s and a series of increasingly refined meshes. Results of these analyses presented in Fig. 15 indicate that the time history of T* was relatively insensitive to mesh refinement for a given height of the exclusion zone. Based on these preliminary calculations, further studies will be conducted in the HSST program on the geometry independence of the (T*, ε) parameter when applied to small- and large-specimen crack run-arrest data.

Moving singular element formulations represent an alternative technique for achieving convergent solutions for fracture parameters in the context of viscoplastic-dynamic fracture analysis. A review of the various computational methods that have employed singular elements in elastodynamic fracture applications is given by Nishioka and Atluri [43]. Two aspects associated with

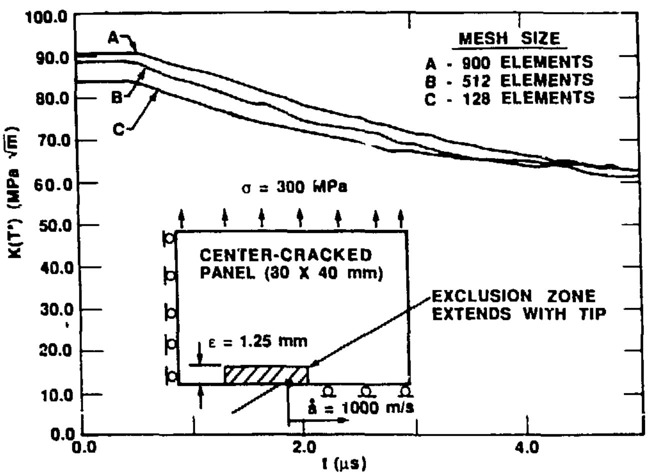

Fig. 15. Comparison of results [$K_I(T^*)$ vs time] from generation-mode viscoplastic-dynamic analyses of center-cracked panel for three mesh refinements and fixed exclusion zone (ε = 1.25 mm).

moving singular element formulations may improve convergence characteristics in inelastic fracture applications. The first is the influence of including singular functions in the solution space of the Ritz-Galerkin approximation. The second, possibly more subtle, aspect is the capability of maintaining a node positioned precisely at the moving discontinuity. (Current nodal relaxation techniques do not specify the exact position of the crack-tip except when the tip is located at an interelement boundary.) In preliminary work, Thesken and Gudmundsson [23] have implemented a variable-order singular element proposed by Akin [44] into an elastodynamic finite-element formulation and have illustrated its advantages in modeling stationary cracks subjected to dynamic loading. More recently, Thesken and Gudmundsson [45] have incorporated a moving element formulation which allows an adjustable region of convecting elements to be embedded at the crack tip within a finite body. The latter technique permits the order of the crack-tip singularity to be specified by an adjustable parameter for dynamic crack growth problems. Applications [45] of this technique have shown good agreement with known analytic solutions of elastodynamic crack growth problems. Work is currently under way in the HSST Program to update the moving element formulation of Thesken and Gudmundsson [45] to accommodate viscoplastic material behavior. The resultant formulation will be investigated for its potential in resolving the near crack-tip singular fields of the Bodner-Partom constitutive model while remaining in the size regime of a continuum element.

3.3 Three-Dimensional Constraint Effects

The finite-element calculations carried out for the wide-plate tests thus far have assumed plane stress conditions over the entire plate. However, in the vicinity of the crack tip, there must be a transition from this plane stress field to a zone dominated by three-dimensional effects. Within this region, the most significant of the three-dimensional effects may be transverse constraint. Insight into the importance of the plane stress vs plane strain issue is found in results reported by Freund and Hutchinson [46] for the extension of their asymptotic analysis of Ref. [41] to plane stress. In that study, the plastic dissipation under plane stress was found to be about two times that under plane strain, all other factors being equal.

Studies being performed by UM on three-dimensional constraint effects are focusing on center-cracked panels, SEN and bend-bar geometries. The SEN and bend-bar analyses have the same specimen geometries and differ only in the applied loading. These studies should provide additional insight into the differences between tensile and moment loading of the crack-tip region. A portion of these results will be employed in the development of techniques for incorporating 3-D constrain effects into 2-D finite element formulations for inelastic-dynamic fracture analysis.

4. CONCLUSION

This paper has summarized recent developments in a coordinated effort being conducted under the HSST Program to develop the crack-arrest data base and the analytical tools required to construct a more comprehensive fracture technology for RPV steels. Because crack initiation is a credible event in a PTS transient, the technology must be available to treat all phases of fracture events. These phases include crack initiation, nonisothermal propagation, arrest, and stable or unstable ductile tearing. The discussion here has focused on analyzing initiation, propagation and arrest of cleavage-fracture behavior.

Experimentally, the crack-arrest data base continues to be enlarged through small- and large-scale experiments performed under the HSST Program. The large-scale wide-plate and PTS experiments are being analyzed using state-of-the-art dynamic analysis techniques. These analyses continue to produce arrest-toughness values that increase at an accelerating rate with temperature near and above the onset of the Charpy upper shelf. In order to construct valid dynamic fracture models for RPV steels, crack run-arrest data corresponding to higher temperature and toughness levels must be generated in greater quantities than can be achieved with large specimens such as wide plates. The intermediate-size stub-panel specimen being developed and tested at ORNL represents a promising technique for substantially augmenting the crack-arrest data base at an affordable cost.

A key component of the fracture technology under development in the HSST Program is evaluating the importance of viscoplastic effects in dynamic fracture analysis. To this end, additional high-strain-rate testing (up to 5000 s^{-1} in shear) has been performed on A533B steel and used to update material constants for the various viscoplastic constitutive models installed in HSST computer programs. The capabilities of these nonlinear techniques are being evaluated, in part, through applications to small- and large-specimen tests, including wide plates. Viscoplastic-dynamic fracture analyses of the wide-plate tests, when expressed in terms of the fracture parameters (T*, etc.), were found to exhibit a strong dependence on mesh refinement. From asymptotic studies of Sheu [24] and Popelar [25], resolution of the crack-tip singular fields in viscoplastic models of engineering structures using conventional finite-element formulations is apparently not within reach currently for practical mesh sizes, even in a supercomputer environment. Even if this resolution were achieved, questions still remain concerning the possible violation of continuum assumptions and the relevance of the proposed parameters (T*, etc.) to predictions of fracture behavior in ductile RPV steel.

Alternative techniques are being investigated in the HSST program to deal with difficulties associated with the small dimensions of the high-strain-rate zones in viscoplastic models. These techniques include a two-component parameter (T*, ε) to exclude the high-strain-rate region from a portion of the calculations and a moving variable-order singular element formulation to build the crack-tip singularity into the finite-element approximation. These techniques will be evaluated separately through analyses of dynamic fracture data from small- and large-specimen crack-arrest experiments.

References

1. B. R. Bass et al., "Fracture Analyses of Heavy-Section Steel Technology Wide-Plate Crack-Arrest Experiments," *Fracture Mechanics: Nineteenth Symposium*, ASTM STP-969, T. A. Cruse (Ed.), pp. 691-733 (1987).

2. M. F. Kanninen and C. H. Popelar, *Advanced Fracture Mechanics*, Oxford University Press, New York, 1985, pp. 214-230.

3. B. Brickstad, "A Viscoplastic Analysis of Rapid Crack Propagation Experiments in Steel," *J. Mech. Phys. Solids*, Vol. 31, pp. 307-27 (1983).

4. R. D. Cheverton et al., "Fracture Mechanics Data Deduced from Thermal-Shock and Related Experiments with LWR Pressure Vessel Material," *Journal of Pressure Vessel Technology*, Vol. 105, pp. 102-110, May 1983.

5. R. H. Bryan et al., "The Heavy-Section Steel Technology Pressurized-Thermal Shock Experiment, PTSE-1," *Eng. Fract. Mech.*, Vol 23(1), pp. 81-97, 1986.

6. R. H. Bryan et al., *Pressurized-Thermal-Shock Test of 6-in. Thick Pressure Vessels. PTSE-2: Investigation of Low Tearing Resistance and Warm Prestressing*, NUREG/CR-4888 (ORNL-6377), Martin Marietta Energy Systems, Inc., Oak Ridge Natl. Lab., January 1988.

7. D. J. Naus et al., *Crack Arrest Behavior in SEN Wide Plates of Quenched and Tempered A533B Steel Tested under Nonisothermal Conditions*, NUREG/CR-4930 (ORNL-6388), Martin Marietta Energy Systems, Inc., Oak Ridge Natl. Lab., September 1987.

8. D. J. Naus et al., "HSST Wide-Plate Test Results and Analysis," *Proceeding of the Sixteenth Water Reactor Safety Research Information Meeting, October 23-27, 1988*, National Bureau of Standards, Gaithersburg, MD (to be published).

9. A. R. Rosenfield et al., "Crack-Arrest Studies at Battelle Columbus," in *HSST Semiannual Progress Report April-September 1984*, NUREG/CR-3744, Vol. 2, (ORNL/TM-9154/V2), pp. 102-109, Martin Marietta Energy Systems, Inc., Oak Ridge National Laboratory, December 1984.

10. J. Keeney-Walker and B. R. Bass, "Analysis of a Stubbed Panel Crack-Arrest Specimen," in *Heavy-Section Steel Technology Program Semiann. Prog. Rep. for April-September 1987*, NUREG/CR-4219, Vol. 4, No. 2 (ORNLTM-9593/V4&N2), Martin Marietta Energy Systems, Inc., Oak Ridge Natl. Lab., April 1988.

11. R. J. Dexter et al., "Dynamic-Viscoplastic Analysis and Small-Specimen Experimental Methods for the Study of Fracture in A533B Steel," in *Proceedings of the Fourth International Conference on Numerical Methods in Fracture Mechanics, March 23-27, 1987, San Antonio, TX.*

12. W. L. Fourney et al., "Investigation of Damping and Cleavage-Fibrous Transition in Reactor-Grade Steel at the University of Maryland," in *Heavy-Section Steel Technology Program Semiann. Prog. Rep. October 1987-March 1988*, NUREG/CR-4219, Vol. 5, No. 1 (ORNL/TM-9593/V5&N1), Martin Marietta Energy Systems, Inc., Oak Ridge Natl. Lab., August 1988.

13. A. Gilat, "High Strain Rate Testing of A533 Grade B Class 1 Steel at Various Temperatures," in *Heavy-Section Steel Technology Program Semiann. Prog. Rep. October 1987-March 1988*, NUREG/CR-4219, Vol. 5, No. 1 (ORNL/TM-9593/V5&N1), Martin Marietta Energy Systems, Inc., Oak Ridge Natl. Lab., August 1988.

14. M. F. Kanninen et al., "Viscoplastic Characterization of A533B Steel," in *Heavy-Section Steel Technology Program Semiann. Prog. Rep. April-September 1986*, NUREG/CR-4219, Vol. 3, No. 2 (ORNL/TM-9593/V3&N2), Martin Marietta Energy Systems, Inc., Oak Ridge Natl. Lab., December 1986.

15. J. H. Giovanola and R. W. Klopp, *Viscoplastic Stress-Strain Characterization of A533B Class 1 Steel*, NUREG/CR-5066 (ORNL/Sub/87-SA193/1), SRI International Menlo Park, CA (to be published).

16. S. R. Bodner and Y. Partom, "Constitutive Equations for Elastic-Viscoplastic Strain Hardening Materials," *J. Appl. Mech.*, 42, 385-389, 1975.

17. P. Perzyna, "Fundamental Problems in Visco-Plasticity," pp. 244-368 in *Recent Advances in Applied Mechanics*, Academic Press, New York, 1966.

18. C. E. Pugh and D. N. Robinson, "Some Trends in Constitutive Equation Model Development for High-Temperature Behavior of Fast-Reactor Structural Alloys," *J. Nucl. Eng. Design*, Vol. 48, No. 1, June 1978, pp. 269-276.

19. K. J. Bathe, *ADINA - A Finite Element Program for Automatic Dynamic Incremental Nonlinear Analysis*, Report AE 84-1, Massachusetts Institute of Technology, Cambridge, MA (December 1984).

20. B. R. Bass et al., "Late-Event Viscoplasticity in Wide-Plate Crack-Arrest Tests," *International Journal of Pressure Vessels and Piping*, Vol. 31, pp. 325-348 (1988).

21. B. R. Bass et al., "Computational Methods for Viscoplastic Dynamic Fracture Mechanics Analysis," *Computers in Engineering 1988*, Vol. 3, (Eds.) V. A. Tipnis and E. M. Patton, ASME, New York (1988).

22. T. Nishioka, "Finite Element Analysis of the T*-Integral in Nonlinear Dynamic Fracture Problems," Proceedings of International Conference on Computational Engineering Science, April 10-14, 1988, Atlanta, GA, pp. 9,V.1-4.

23. J. C. Thesken and P. Gudmundsson, "Application of a Variable Order Singular Element to Dynamic Fracture Mechanics," *Computational Mechanics*, Vol. 2, pp. 307-316 (1987).

24. J. C. Sheu, "Dynamic Elastic-Viscoplastic Crack Growth," Ph.D. Dissertation, School of Engineering, Ohio State University, 1988.

25. C. H. Popelar, "A Viscoplastic Analysis for Predicting the Dynamic Fracture Toughness of A533B Steel," submitted for publication.

26. C. F. Fedderson, *Current Status of Plane Strain Crack Toughness Testing of High-Strength Metallic Materials*, Crack Arrest Methodology and Applications, ASTM STP-410, American Society for Testing and Materials, Philadelphia, PA, 1967.

27. R. Tada, P. C. Paris, and G. R. Irwin, *The Stress Analysis of Cracks Handbook*, Del Research Corp., Hellertown, PA.

28. C. W. Schwartz, "Dynamic Fracture Propagation Relations Inferred from WP-1 Test Series," in *Heavy-Section Steel Technology Program Semiann. Prog. Rep. for April-September 1987*, NUREG/CR-4219, Vol. 4, No. 2 (ONRL/TM-9593/V4&N2), Martin Marietta Energy Systems, Inc., Oak Ridge Natl. Lab., April 1988.

29. B. R. Bass, C. E. Pugh, and J. K. Walker, "Elastodynamic Fracture Analysis of Large Crack-Arrest Experiments," *Nuclear Engineering and Design*, Vol. 98, 157-169, 1987.

30. C. E. Pugh et al., "Evaluation of Crack-Arrest Toughness through Dynamic Fracture Analysis of Large Vessel Tests," *Proceedings of the Seventh International Conference on Fracture, March 20-24, 1989, Houston, TX*, to be published.

31. M. F. Kanninen, "Elastodynamic and Viscoplastic-Dynamic Fracture Mechanics," in *Heavy-Section Steel Technology Program Semiann. Prog. Rep. October 1987-March 1988*, NUREG/CR-4219, Vol. 5, No. 1 (ORNL/TM-9593/V5&N1), Martin Marietta Energy Systems, Inc., Oak Ridge Natl. Lab., August 1988.

32. L. Dahlberg et al., "Influence of Specimen Geometry on Crack Propagation and Arrest Toughness," *Crack Arrest Methodology and Applications*, ASTM STP-711, G. T. Hahn and M. F. Kanninen (Eds.), pp. 89-108 (1980).

33. S. N. Atluri, T. Nishioka, and M. Nakagaki, "Incremental Path Independent Integrals in Inelastic and Dynamic Fracture Mechanics," *Eng. Fract. Mech.*, Vol. 20-2, pp. 209-244 (1984).

34. K. Kishimoto, S. Aoki, and M. Sakata, "On the Path-Independent Integral $-\hat{J}$," *Eng. Fract. Mech.*, Vol. 13, pp. 841-50 (1980).

35. S.-J. Chang, "ORNL Unified Inelastic Deformation Model," in *Heavy-Section Steel Technology Program Semiann. Prog. Rep. October 1987-March 1988*, NUREG/CR-4219, Vol. 5, No. 1 (ORNL/TM-9593/V5&N1), Martin Marietta Energy Systems, Inc., Oak Ridge Natl. Lab., August 1988.

36. S.-J. Chang, *Inelastic Analysis and Testing of SUS 304 Stainless Steel*, by J. J. Blass et al., EPRI 2658-21, pp. 38-43, EPRI, Palo Alto, Calif., 1988.

37. K. Hornberger et al., "Numerical Integration and Implementation of Viscoplastic Models into Finite Element Codes," pp. 477-90, *Proc. of Third International Conference on Computational Plasticity, Barcelona, Spain, April 6-10, 1987*, Pineridge Press, Swansea, U.K.

38. B. Brickstad, *Wide-Plate Analysis of WP-1.2 and WP-1.5*, presented at the Third Annual HSST Workshop on Crack Arrest Technology, National Bureau of Standards, Gaithersburg, MD, May 1987.

39. B. R. Bass et al., *Viscoplastic Dynamic Fracture Analyses of the WP-1 Series of Wide Plate Crack-Arrest Tests*, ORNL/TM- , Martin Marietta Energy Systems, Inc., Oak Ridge Natl. Lab., to be published.

40. J. Ahmad, "Elastic-Viscoplastic Analysis of Rapidly Running Cracks," *Proc. of Fourth International Conference Numerical Methods in Fracture Mechanics*, March 23-27, 1987, San Antonio, TX.

41. L. B. Freund and J. W. Hutchinson, "High Strain-Rate Crack Growth in Rate-Dependent Plastic Solids," *J. Mech. Phys. Solids*, Vol. 33, No. 2, pp. 169-191 (1985).

42. P. O'Donoghue, "Crack-Tip Characterizing Parameters in Dynamic Visco-plastic Fracture Mechanics", *Fourth Annual HSST Program Workshop on Dynamic Fracture and Crack Arrest Technology, June 2-3, 1988, National Bureau of Standards, Gaithersburg, MD.*

43. T. Nishioka and S. N. Atluri, "Computational Methods in Dynamic Fracture," in *Computational Methods in the Mechanics of Fracture*, (Ed.) S. N. Atluri, North Holland, Amsterdam (1986).

44. J. E. Akin, "The Generation of Elements with Singularities," *Int. J. Num. Meth. Eng.*, Vol. 10, pp. 1249-1259 (1976).

45. J. C. Thesken and P. Gudmundsson, "Application of a Moving Variable Order Singular Element to Dynamic Fracture Mechanics," to be published.

46. J. W. Hutchinson, Letter Report on the 3rd HSST Workshop on Dynamic Fracture and Crack Arrest, to C. E. Pugh, Heavy-Section Steel Technology Program, Oak Ridge Natl. Lab., July 1, 1987.

ORNL-WSC-6813 ETD

ADVANCES IN CRACK-ARREST TECHNOLOGY FOR REACTOR PRESSURE VESSELS

B. R. BASS
C. E. PUGH
Heavy Section Steel Technology Program
Oak Ridge National Laboratory

presented at
16th Water Reactor Safety Information Meeting
Gaithersburg, Maryland

October 24-27, 1988

ornl

MOTIVATION FOR FURTHER DEVELOPMENT OF FRACTURE ASSESSMENT CAPABILITIES IS DERIVED FROM IMPORTANT SAFETY-RELATED OBJECTIVES OF THE NRC

- TO PROVIDE THE BEST POSSIBLE ESTIMATE OF RISK ASSOCIATED WITH PTS SCENARIOS
- TO PROVIDE AN INDEPENDENT UNDERSTANDING OF THE LEVELS OF CONSERVATISM IN CURRENT RULES AND REGULATIONS PERTAINING TO PTS SCENARIOS
- TO INCORPORATE THE CONCEPT OF CRACK INITIATION, PROPAGATION, AND ARREST AS CREDIBLE EVENTS IN PTS SCENARIOS

THE ESSENTIAL FEATURES OF THE FRACTURE ASSESSMENT TECHNOLOGY CURRENTLY UNDER DEVELOPMENT REFLECT SEVERAL IMPORTANT FACTORS

- ASSESSMENT OF VESSEL INTEGRITY REQUIRES ABILITY TO PREDICT ALL PHASES OF DYNAMIC FRACTURE EVENTS
- TECHNOLOGY MUST INCLUDE DYNAMIC STRESS-ANALYSIS METHODS, FRACTURE MODELS, CRITERIA, AND DATA CURVES
- TECHNOLOGY MUST BE DEVELOPED AND VALIDATED THROUGH LARGE- AND SMALL-SPECIMEN EXPERIMENTS
- DEVELOPMENT IS BEING ACCOMPLISHED THROUGH INTEGRATED EFFORTS OF SEVERAL RESEARCH LABORATORIES AND UNIVERSITIES

THE HSST PROGRAM IS MEETING THE NEED BY DEVELOPING A COMPREHENSIVE DYNAMIC-FRACTURE ASSESSMENT TECHNOLOGY THAT ACCOMMODATES SEVERAL IMPORTANT TECHNICAL ISSUES

- STRAIN-RATE-DEPENDENT (I.E., VISCOPLASTIC) DATA AND CONSTITUTIVE MODELS
- FINITE-ELEMENT COMPUTER PROGRAMS FOR DYNAMIC STRUCTURAL ANALYSIS
- CRACK INITIATION/PROPAGATION/ARREST DATA AND INTERPRETATIONS
- DYNAMIC FRACTURE MODELS FOR CHARACTERIZING FRACTURE BEHAVIOR

ORNL-DWG88-4455 ETD

BECAUSE HIGH STRAIN RATES (~10^4 s^{-1}) ARE PRESENT IN THE VICINITY OF A FAST-RUNNING CRACK, THE STRAIN-RATE-DEPENDENT BEHAVIOR OF RPV STEELS MUST BE INCLUDED IN DYNAMIC INELASTIC FRACTURE MODELS

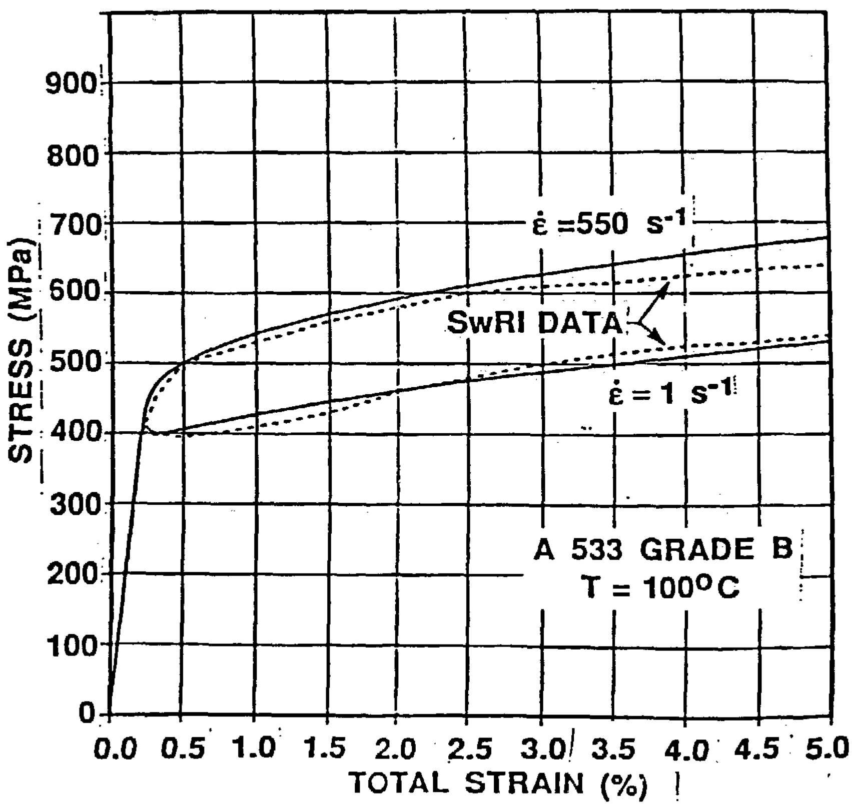

ornl

VISCOPLASTIC FRACTURE MODELS CAN REMOVE GEOMETRY DEPENDENCE IN LEFM-DERIVED FRACTURE TOUGHNESS RELATIONS FOR STRAIN-RATE SENSITIVE STEELS

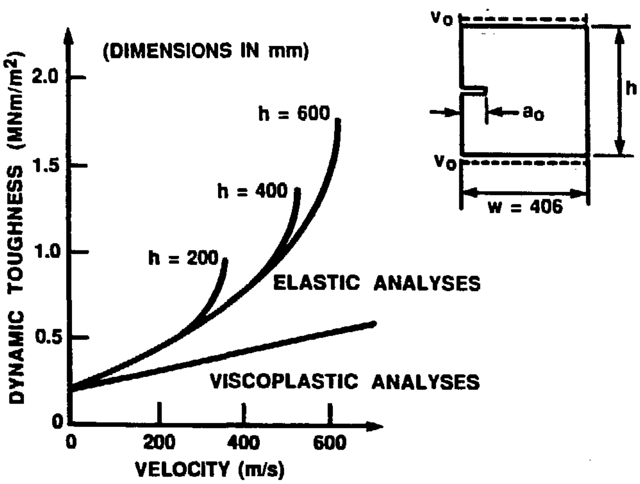

ornl

MARTIN MARIETTA

MARTIN MARIETTA ENERGY SYSTEMS, INC

BRB-4

FRACTURE MODELS THAT INCORPORATE PLASTICITY AND STRAIN-RATE EFFECTS ARE BEING DEVELOPED IN THE HSST PROGRAM THROUGH COORDINATED EFFORTS OF SEVERAL ORGANIZATIONS

- VISCOPLASTIC TESTS OF RPV STEELS AT STRAIN RATES UP TO 5000 s^{-1} AND TEMPERATURES FROM -150°C TO 300 °C (OSU, SWRI, SRI)
- DETERMINATION OF MATERIAL CONSTANTS FOR VISCOPLASTIC CONSTITUTIVE MODELS FROM HIGH-STRAIN-RATE DATA (ORNL, SWRI, UM, NORDIC)
- DEVELOPMENT OF VISCOPLASTIC-DYNAMIC, FINITE-ELEMENT FRACTURE TECHNIQUES (ORNL, OSU, SWRI, UM, NORDIC)
- PERFORMANCE AND ANALYSIS OF SMALL- AND LARGE-SPECIMEN TESTS FOR VALIDATION OF FRACTURE MECHANICS MODELS (ORNL, SWRI, UM, NORDIC)

SEVERAL VISCOPLASTIC CONSTITUTIVE MODELS AND INELASTIC FRACTURE CRITERIA ARE EVALUATED ON THE BASIS OF THEIR ABILITY TO PREDICT FRACTURE EXPERIMENTS

- FINITE-ELEMENT COMPUTER PROGRAMS ARE USED TO EVALUATE INELASTIC METHODOLOGIES
- THREE VISCOPLASTIC CONSTITUTIVE MODELS HAVE BEEN IMPLEMENTED
  - BODNER-PARTOM (WITH STRAIN HARDENING)
  - PERZYNA (WITH LINEAR STRAIN HARDENING)
  - ROBINSON (WITH ISOTROPIC AND KINEMATIC HARDENING)
- THREE PROPOSED INELASTIC FRACTURE CRITERIA HAVE BEEN IMPLEMENTED
  - T^* (ATLURI)
  - $\hat{J}$ (KISHIMOTO)
  - γ (BRICKSTAD)

ornl

THE HSST PROGRAM IS MEETING THE NEED BY DEVELOPING A COMPREHENSIVE DYNAMIC-FRACTURE ASSESSMENT TECHNOLOGY THAT ACCOMMODATES SEVERAL IMPORTANT TECHNICAL ISSUES

- STRAIN-RATE-DEPENDENT (I.E., VISCOPLASTIC) DATA AND CONSTITUTIVE MODELS
- FINITE-ELEMENT COMPUTER PROGRAMS FOR DYNAMIC STRUCTURAL ANALYSIS
- CRACK INITIATION/PROPAGATION/ARREST DATA AND INTERPRETATIONS
- DYNAMIC FRACTURE MODELS FOR CHARACTERIZING FRACTURE BEHAVIOR

TWO COMPUTER PROGRAMS HAVE BEEN INDEPENDENTLY DEVELOPED TO COMPARE SELECTED COMPUTATIONAL METHODS

- ADINA/VPF WAS DEVELOPED BY ORNL AND UM FROM THE ADINA GENERAL-PURPOSE PROGRAM (DISPLACEMENT-BASED FORMULATION)
- VISCRK WAS DEVELOPED BY SWRI SPECIALLY FOR VISCOPLASTIC-DYNAMIC FRACTURE (RATE-DEPENDENT FORMULATION)
- COMPARATIVE FRACTURE ANALYSES HAVE BEEN PERFORMED TO VERIFY THE PROGRAMS

THE HSST PROGRAM IS MEETING THE NEED BY DEVELOPING A COMPREHENSIVE DYNAMIC-FRACTURE ASSESSMENT TECHNOLOGY THAT ACCOMMODATES SEVERAL IMPORTANT TECHNICAL ISSUES

- STRAIN-RATE-DEPENDENT (I.E., VISCOPLASTIC) DATA AND CONSTITUTIVE MODELS
- FINITE-ELEMENT COMPUTER PROGRAMS FOR DYNAMIC STRUCTURAL ANALYSIS
- CRACK INITIATION/PROPAGATION/ARREST DATA AND INTERPRETATIONS
- DYNAMIC FRACTURE MODELS FOR CHARACTERIZING FRACTURE BEHAVIOR

ornl

ORNL-DWG88-3899A ETD

DATA FOR "DEVELOPMENT" OF DYNAMIC-FRACTURE MACHANICS MODELS ARE GENERATED FROM A VARIETY OF SMALL-SPECIMEN TESTS

SMALL-SPECIMEN TESTS

GENERATION-PHASE ANALYSIS

DYNAMIC FRACTURE TOUGHNESS MODEL

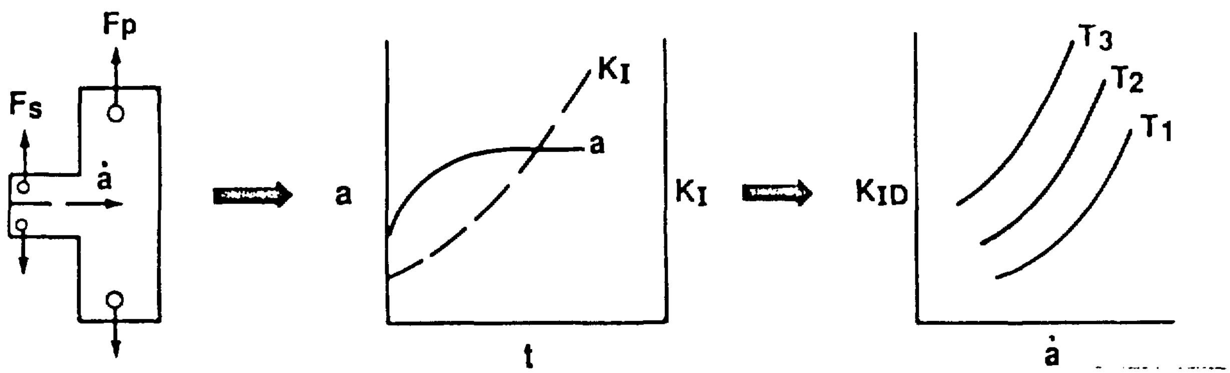

DATA FOR "VALIDATION" OF DYNAMIC-FRACTURE MACHANICS MODELS ARE GENERATED FROM LARGE-SPECIMEN TESTS

LARGE-SPECIMEN TESTS (WIDE-PLATE, ETC.)

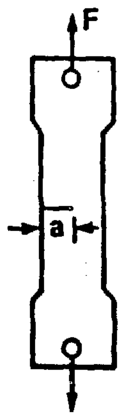

⟹

APPLICATION-PHASE ANALYSIS

$K_{I\text{-APPLIED}} = K_{ID}(\dot{a}, T)$

⇓

$\dot{a}(t)$

⟹

CRACK-RUN ARREST PREDICTIONS

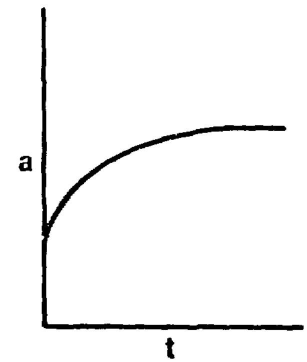

ornl

Baer (14)

ORNL-DWG87-4891A ETD

RESULTS FROM THE SIXTEEN HSST WIDE-PLATE TESTS HAVE BEEN USED IN DYNAMIC FRACTURE TOUGHNESS ASSESSMENTS

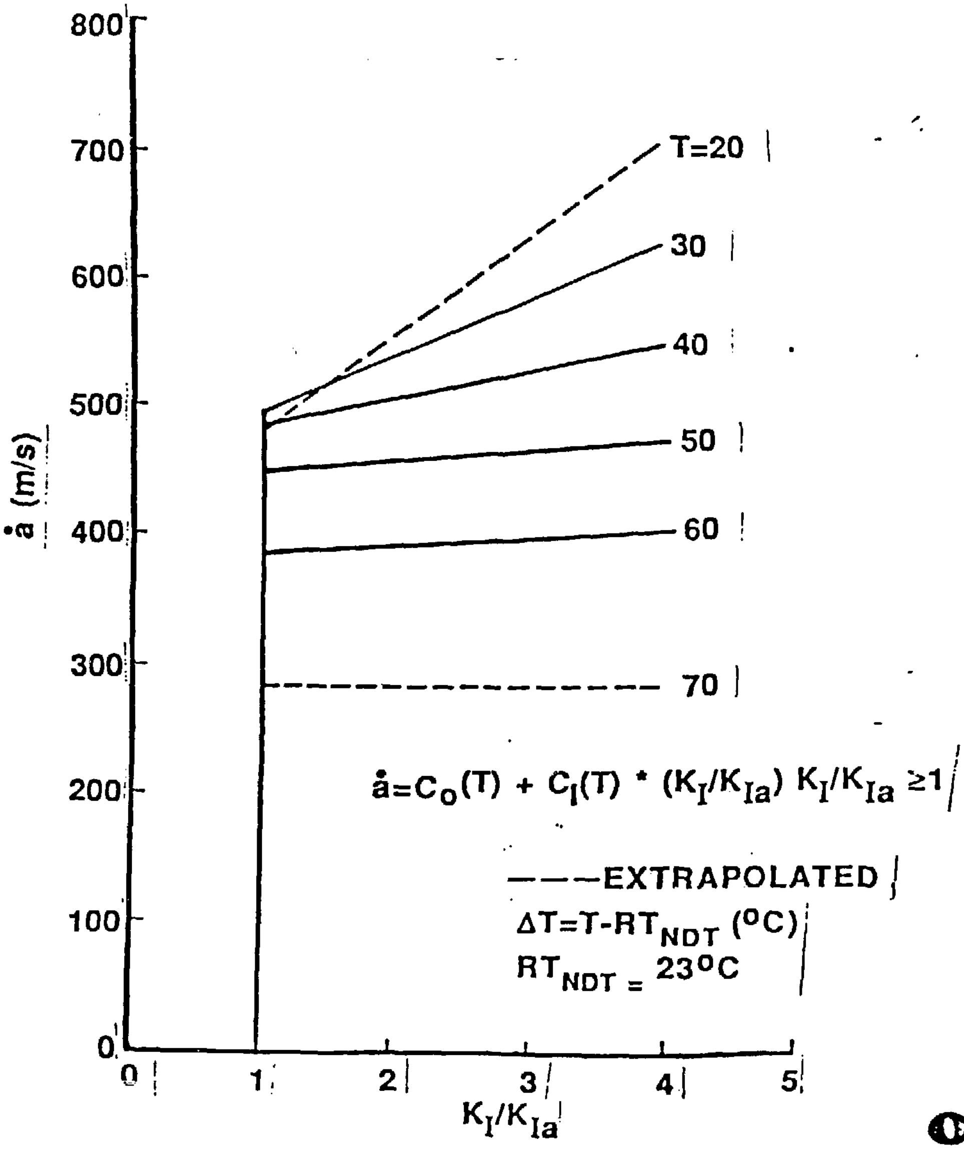

ornl

ORNL-DWG 88-4816 ETD

DYNAMIC ANALYSIS METHODS MUST BE EMPLOYED TO ACCURATELY INTERPRET CRACK PROPAGATION-ARREST DATA FROM LARGE-SCALE WIDE-PLATE TESTS

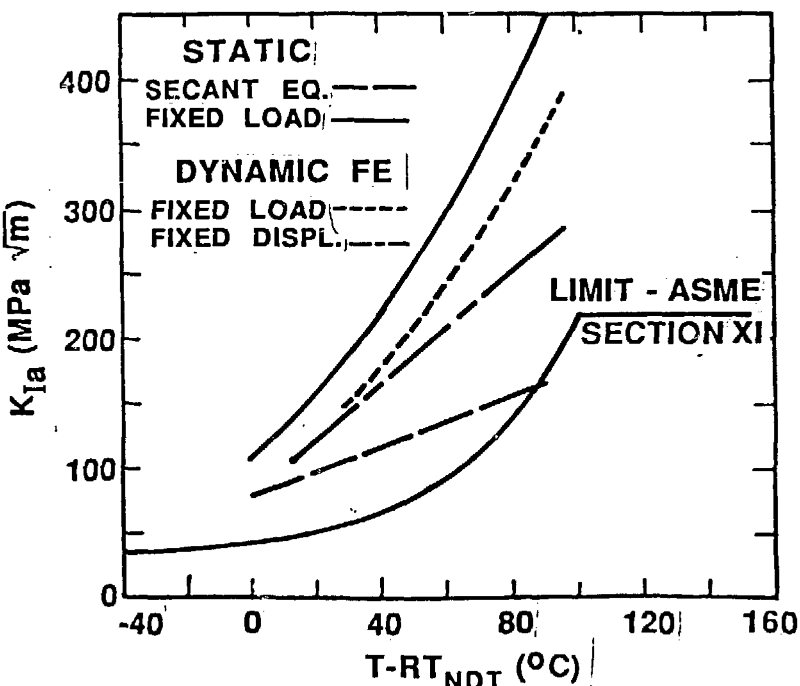

ornl

ORNL-DWG87-4981B ETD

LARGE-SPECIMEN DATA AND DYNAMIC ANALYSIS RESULTS FOR WIDE-PLATE TESTS EXHIBIT A CONSISTENT TREND IN ARREST TOUGHNESS ABOVE THE ASME LIMIT

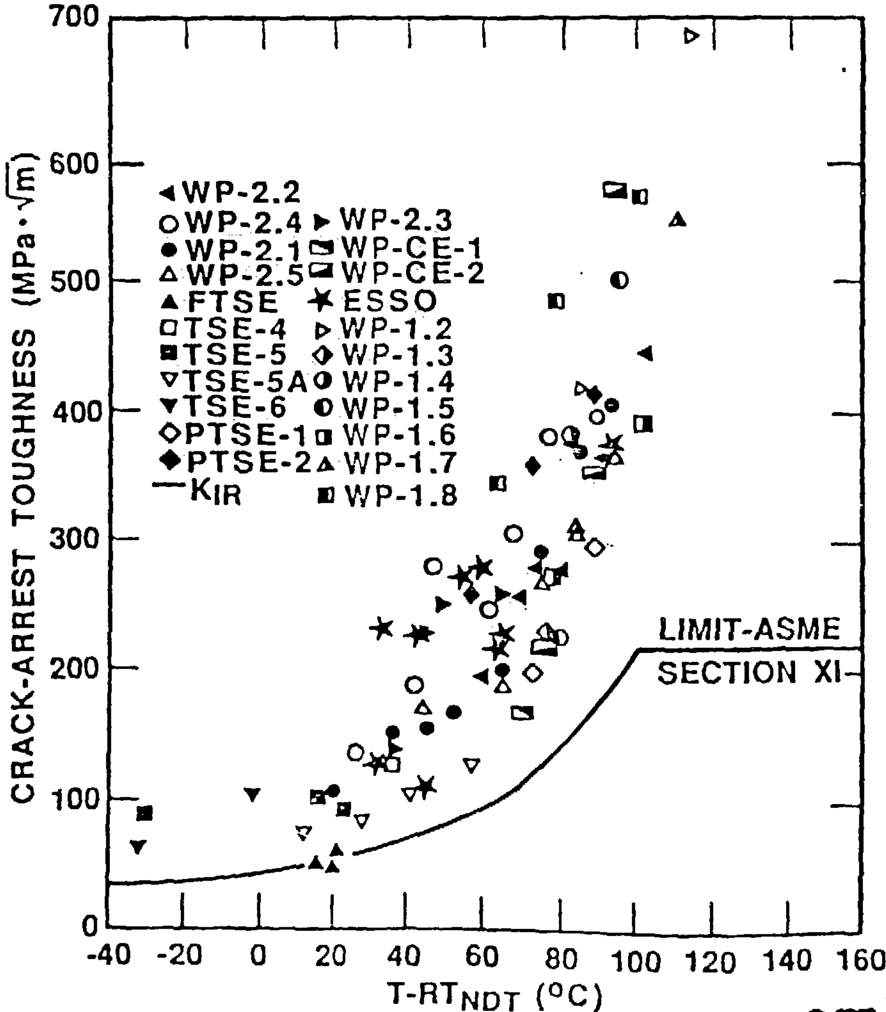

ornl

THE HSST PROGRAM IS MEETING THE NEED BY DEVELOPING A COMPREHENSIVE DYNAMIC-FRACTURE ASSESSMENT TECHNOLOGY THAT ACCOMMODATES SEVERAL IMPORTANT TECHNICAL ISSUES

- STRAIN-RATE-DEPENDENT (I.E., VISCOPLASTIC) DATA AND CONSTITUTIVE MODELS
- FINITE-ELEMENT COMPUTER PROGRAMS FOR DYNAMIC STRUCTURAL ANALYSIS
- CRACK INITIATION/PROPAGATION/ARREST DATA AND INTERPRETATIONS
- DYNAMIC FRACTURE MODELS FOR CHARACTERIZING FRACTURE BEHAVIOR

ORNL-DWG 88-4829 TD

VISCOPLASTIC-DYNAMIC SOLUTIONS OF WIDE-PLATE TESTS FROM CONVENTIONAL FINITE ELEMENT FORMULATIONS ARE NOT CONVERGENT FOR PRACTICAL MESH REFINEMENTS

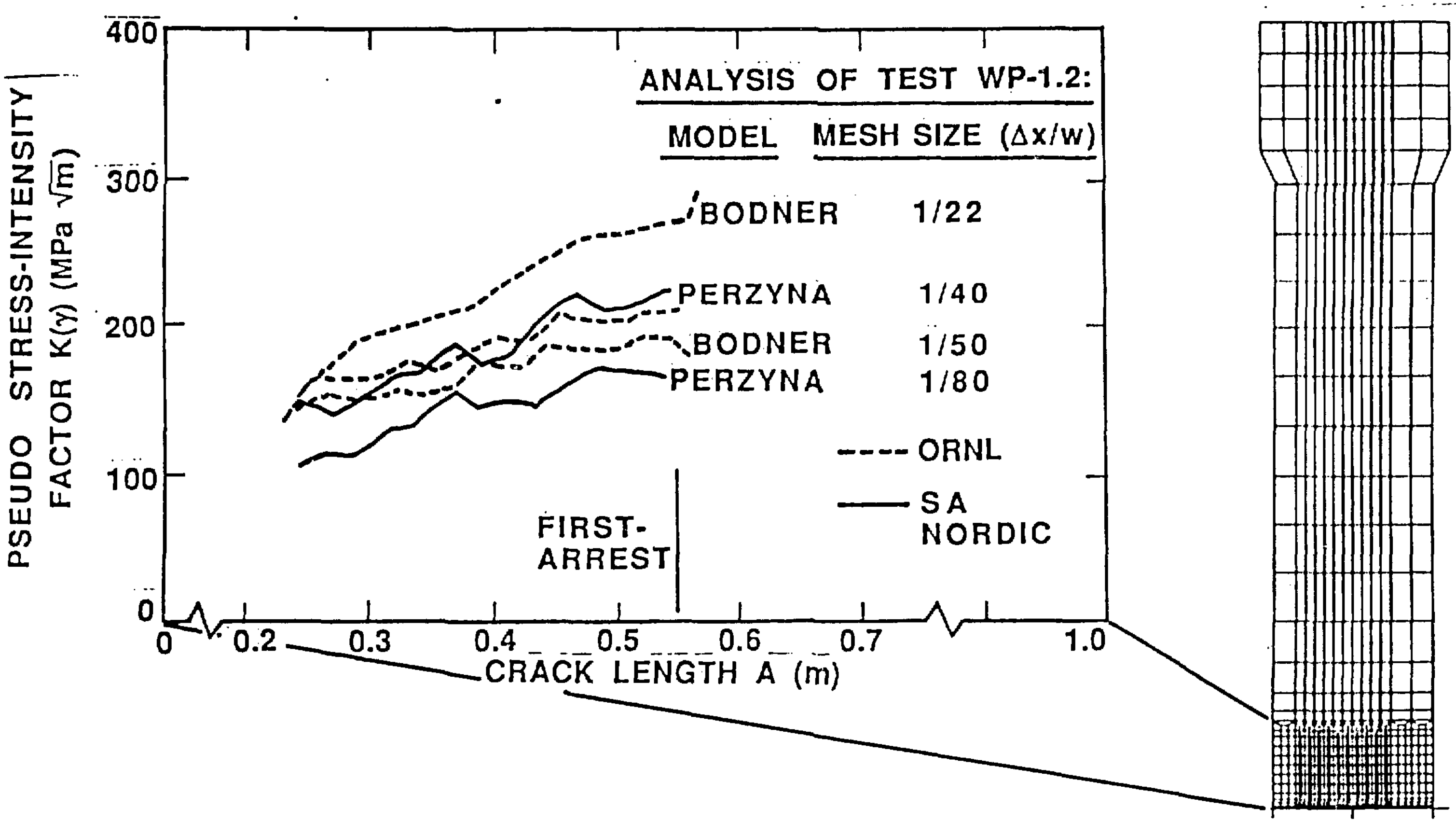

ornl

ORNL-DWG88-4815 ETD

RECENT ASYMPTOTIC STUDIES (OSU AND NORDIC) INDICATE HIGH STRAIN-RATE ZONE OF DOMINANCE IS VERY SMALL (ORDER 10^{-3}) COMPARED TO SIZE OF INELASTIC REGION

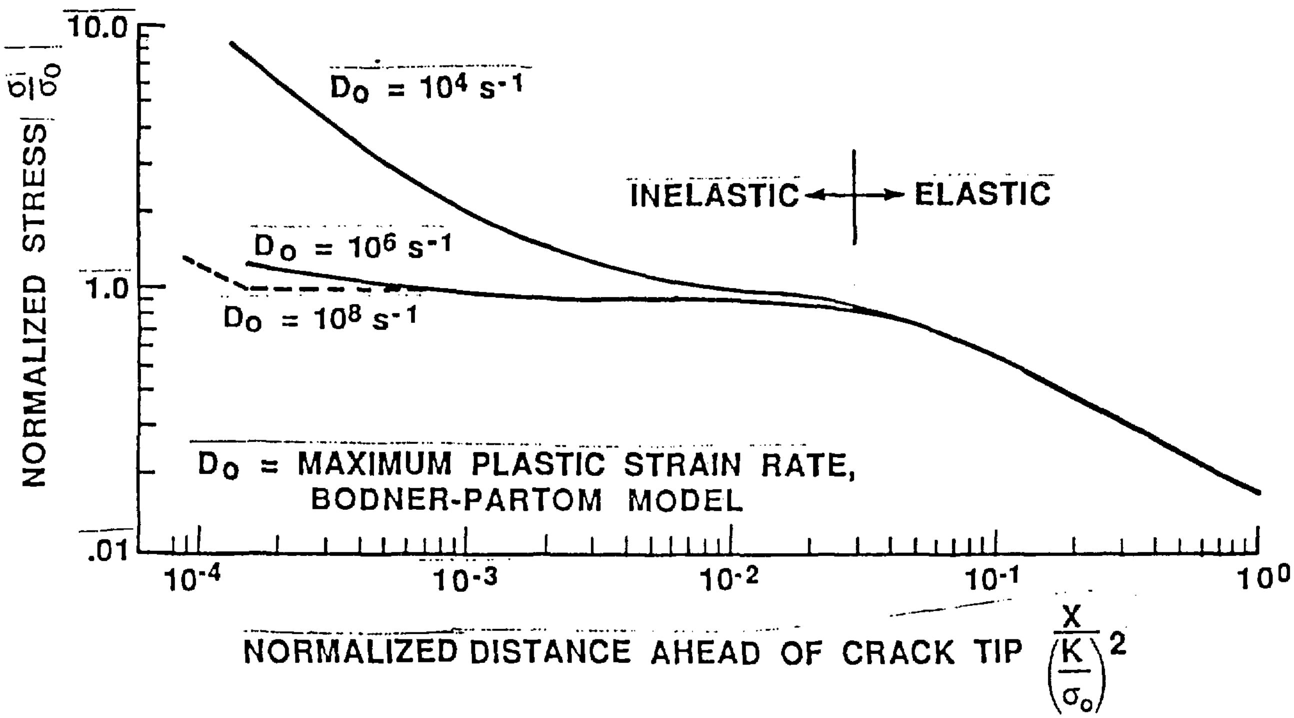

THE TWO-COMPONENT EXCLUSION-ZONE PARAMETER (T*,ε) IS BEING EVALUATED BY SWRI FOR POTENTIAL USE IN INELASTIC FRACTURE MODELS

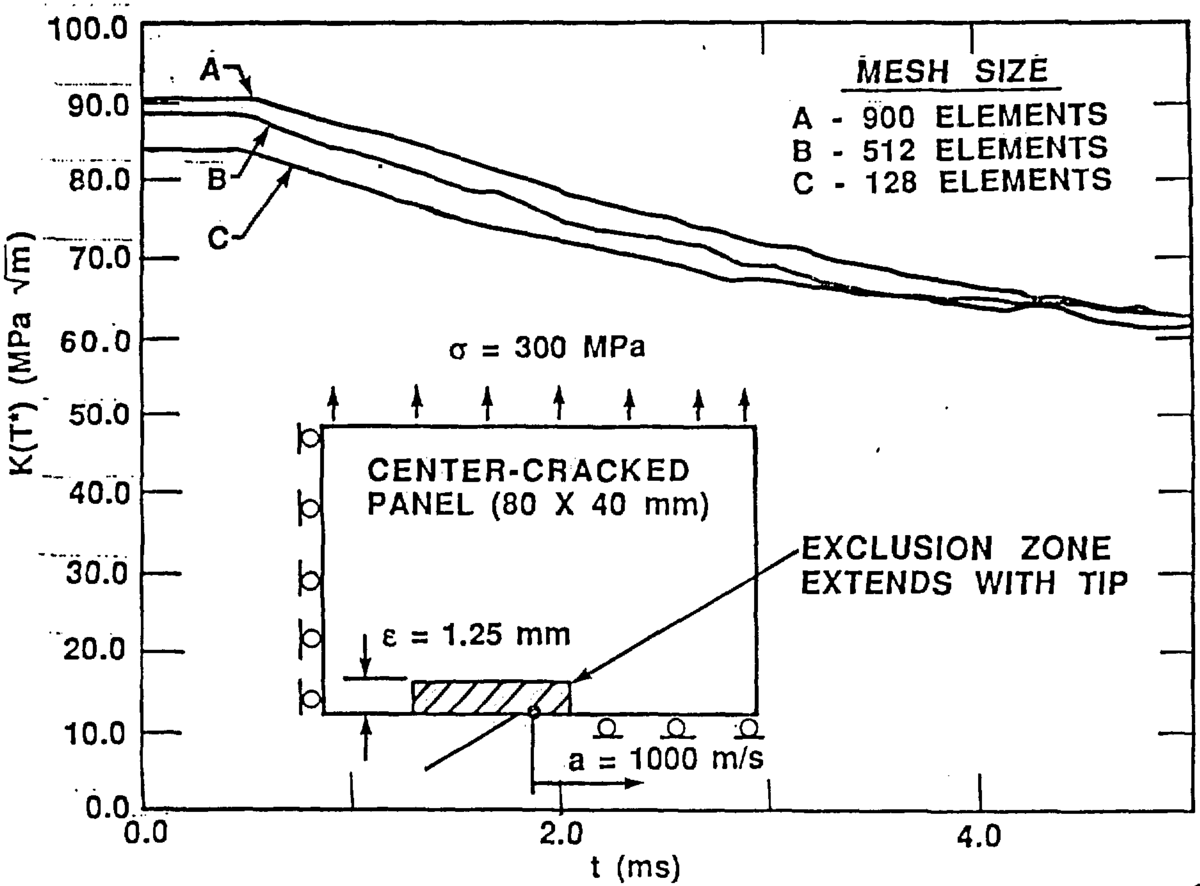

ORNL-DWG 88-4826 ETD

MOVING VARIABLE-ORDER SINGULAR ELEMENTS ARE BEING EVALUATED BY ORNL FOR POTENTIAL USE IN MODELING NEAR CRACK-TIP HIGH STRAIN-RATE ZONES

- ADJUSTABLE SINGULARITY BUILT INTO CRACK-TIP ELEMENT
- ELEMENTS TRANSLATE TO MODEL CRACK-TIP POSITION
- METHOD EMBEDDED IN REGULAR FEM PROGRAM

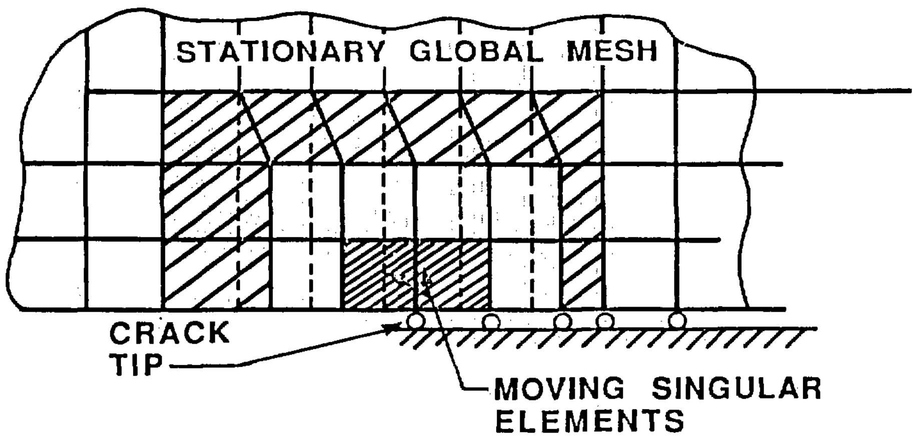

ornl

IN CONCLUSION, HSST STUDIES ARE PROGRESSING TOWARD DEVELOPMENT OF A DYNAMIC-INELASTIC, FRACTURE-MECHANICS MODEL FOR RPV STEELS

- APPLYING STATE-OF-THE-ART FRACTURE ANALYSIS METHODS TO CURRENT HSST EXPERIMENTS
- DEVELOPING CONVERGENT ANALYSIS METHODS FOR CRACK PROPAGATION EVENTS (MOVING SINGULAR ELEMENTS, ETC.)
- INVESTIGATING PROPOSED PARAMETERS (T*, ε, ETC.) FOR CHARACTERIZING FRACTURE BEHAVIOR
- INCORPORATING THREE-DIMENSIONAL EFFECTS INTO CRACK-TIP DEFORMATION ANALYSIS
- DEVELOPING AND VALIDATING MODELS THROUGH ANALYSIS OF ADDITIONAL SMALL- AND LARGE-SPECIMEN TESTS